# Abstract

McDANIEL, MATTHEW CARY. Characterizing Individual Response to Lipid Infusions using Time-Varying Physiological Parameters to Predict Lipid Resuscitation Outcomes. (Under the direction of Dr. Kevin Flores.)

Local anesthetic systemic toxicity (LAST) is a life-threatening event in which the introduction of anesthetic to the bloodstream induces rapid onset of cardiac arrest. The severity of this condition is compounded by its resistance to traditional methods of resuscitation. A potential remedy emerged twenty years ago when it was observed that injecting rats with the solution Intralipid decreased their susceptibility to toxic events caused by the anesthetic bupivacaine. The widespread clinical availability of Intralipid made this phenomenon all the more intriguing. Momentum behind Intravenous Lipid Emulsion (ILE) therapy built following further studies in animals and crescendoed in the mid-2000s when it was implicated in the rescue of several patients from LAST.

Encouraging as some case studies have been, a contingent of the medical community has expressed concern that positive reports have led to adoption of ILE therapy without proper validation of its efficacy. They argue out that the biological mechanism by which ILE therapy operates has not been fully elucidated and that the proposed "lipid sink" theory cannot adequately explain all experimental observations. Furthermore, they point to experiments in other animals that have produced conflicting results with respect to the superiority of ILE therapy over traditional resuscitation techniques. This opposition desires not to debunk ILE therapy, but to ensure that physicians understand when it is appropriate to use it. This point is particularly critical when considering that ILE therapy has already been attempted in oral rather than intravenous overdose cases, as well as in cases involving drugs other than lipid-based local anesthetics.

The purpose of our study was twofold. We first sought to demonstrate how mathematical analysis can be used to gain insight into the mechanism by which ILE therapy operates. In doing so, we establish how estimation of relevant physiological parameters on an individual basis can inform personal treatment protocols and establish population level trends. Using data previously collected in a study involving rats, we identified two key parameters in a compartmental, physiologically-based pharmacokinetic/pharmacodynamic (PK/PD) model associated with lipid interactions that can be estimated for each subject. One parameter was determined to be correlated with the magnitude of cardiac response to lipid infusion, while the other played a role in determining the smoothness of the response. To account for the dynamic nature of the process, we adjusted the PK/PD model to allow time variation in our selected parameters using one, four, or eight linear splines of equal length. We evaluated the quality of our candidate models with model comparison nested restraint tests and Akaike Information Criteria (AIC), determining that a model with four linear splines was most appropriate for our data set. We constructed population distributions for each parameter using the individual estimates, sampling from them repeatedly to create a virtual population undergoing ILE therapy in response to a simulated overdose of the anesthetic bupivacaine. The virtual population exhibited a wide range of expected outcome, demonstrating how the viability of ILE therapy could depend strongly on the individual.

Future work will seek to expand the pool of parameters we are able to estimate to increase the confidence which we can place on our virtual populations. Transitioning our study to higher animal models is another logical step forward. We are confident that by doing so we will contribute to the understanding of ILE therapy and provide a blueprint for characterizing treatment on an individual basis.

# Characterizing Individual Response to Lipid Infusions using Time-Varying Physiological Parameters to Predict Lipid Resuscitation Outcomes

by
Matthew Cary McDaniel

A thesis submitted to the Graduate Faculty of
North Carolina State University
in partial fulfillment of the
requirements for the Degree of
Master of Science

Biomathematics

Raleigh, North Carolina

2017

APPROVED BY:

| | |
|---|---|
| Belinda Akpa | Hien Tran |

Kevin Flores
Chair of Advisory Committee

# Biography

Matthew McDaniel was born in Phoenix, AZ. His parents loved him, so they moved to Tucson rather than allow Matthew to suffer the ignominy of growing up an Arizona State fan.

# Acknowledgments

Thanks to Dr. Kevin Flores and Dr. Belinda Akpa for the opportunity to work on this project and for all their support. Specifically, I'd like to acknowledge all the great input I got from Kevin relating to the mathematical execution of our study and for being available to talk at the drop of a hat. Dr. Akpa was instrumental in the process of transferring the PK/PD model to a Matlab format that we could use to perform our study. She also provided the data which we used for this study and was an excellent resource on questions relating to the physiological and medical interpretation of our work.

# Table of Contents

# List of Tables

# List of Figures

# 1 Review

## 1.1 Development of ILE Therapy

The use of local anesthesia is an established operating procedure in clinical settings. Local anesthetics–which come in the form of topical applications, local infiltration, and nerve blocks[28]-very rarely produce adverse side effects. Yet when they do, the risk to a patient's life is extreme. If a local anesthetic enters bloodstream, usually by inadvertent infusion, central nervous system and cardiac toxicity can result [41]. The severity of local anesthetic system toxicity (LAST), as it is called, stems from its strong negative inotropic effect on the heart [6]. That is, LAST weakens the cardiac muscle tissue.

To further complicate matters, individuals experiencing LAST do not respond well to traditional resuscitation methods [46]. Concern over this issue was first brought to light by Stephen Albright of Stanford Medical Center in 1979. Albright expressed doubts that standard resuscitation protocol could mitigate cardiac arrest induced by "potent, highly lipid soluble and protein-bound amide...agents such as etidocaine and bupivacaine" [1]. Yet in the absence of a realistic alternative, the agents referenced by Albright remain widely used. As of 2013, estimated incidence of LAST was 0.87 out of 1000 patients [5].

Interestingly, the lipophillic property cited by Albright as playing a role in LAST might hold the key to combating it. Weinberg et al observed in 1998 that the mean lethal dosage of bupivacaine required to induce asystole [i.e. flat-line] in rats could be increased by pre-treating the animals with an intravenously injected lipid emulsion [53]. The solution in question was Intralipid, which is commonly used as a source of free fatty acids in parenteral nutrition [49]. Weinberg postulated that the Intralipid acts as a sink for the highly lipid soluble anesthetic, lowering its concentration in the plasma

[53]. *In vitro* experiments appeared to support this lipid sink theory, as the lipid:aqueous partition coefficient for bupivacaine was found to be 11.9. In a follow-up study performed with dogs, all animals treated with Intralipid survived bupivacaine-induced cardiotoxity compared to none in the control group [52]. At this juncture, an editorial raised the question of whether Intravenous Lipid Emulsion (ILE) therapy might represent the "silver bullet" in treating LAST [50].

Enthusiasm heightened in 2006 when ILE therapy was successfully applied for the first time in a clinical setting [45]. A male patient went into cardiac arrest after receiving bupivacaine and, after 20 minutes of standard resuscitation protocol, could not be revived. The patient was given a 100 mL bolus infusion of 20% Intralipid and, within seconds, began showing signs of recovery. Further stabilization of the patient was achieved by administering a continuous infusion of lipid. Over the next several years, subsequent case studies were published describing reversal of cardiac toxicity brought about by a range of anesthetics, including levobupivacaine [18], mepivacaine [34], prilocaine [34], ropivacaine [35], and lidocaine [35]. In each case, reversal was accomplished using a regimen of a bolus infusion of lipid followed by a continuous infusion.

Each documented rescue event has been received by many as more evidence in favor of the "silver bullet". ILE therapy has gained recognition from such medical societies as the American Heart Association and the American College of Medical Toxicology, which now list recommendations for when and how to administer ILE therapy [3], [2]. Some medical professionals have begun promoting ILE therapy as a first defense again LAST rather than as a last resort. Others have attempted ILE therapy in response to both oral and intravenous overdose of other lipophilic drugs such as antidepressant, antipsychotics, calcium channel blockers, and antiarrhythmics [20].

## 1.2 Controversy Concerning ILE

### 1.2.1 Mechanism

Though ILE therapy certainly shows promise, some worry that clinicians and researchers have been too quick to endorse and expand it without full consideration of its efficacy. Troubling to many is the fact that the mechanism by which lipid emulsions detoxify cardiac tissue has not been fully elucidated. True, the "lipid sink" theory has been repeatedly cited owing to the high binding coefficients recorded *in vitro* between Intralipid and many lipophilic anesthetics [38]. However, some experiments have shown ILE to be capable of inducing a physiological response on a faster time scale than what should be expected under the assumption of the lipid sink, implying that alternative mechanisms could be at work [46]. These other mechanisms can be grouped into metabolic effects, positive inotropy, and ion channel regulation.

The proposed metabolic effect considers that lipid acts as a source of free fatty acids. During stunned myocardium (contractile abnormalities in the heart), the rate of fatty acid oxidation decreases, leading to reduced intracelluar ATP levels [11]. It therefore seems plausible that by-passing fatty acid oxidation by direct infusion of free lipids might promote cardiac recovery. De Velde studied this possibility by inducing stunned myocardium in dogs and treating them with either a saline control or Intralipid [11]. The Intralipid treatment group showed faster recovery of normal function than did the control group. However, these effects were mitigated when oxfenicine, an inhibitor of free fatty acid metabolism in myocardial tissue, was supplied with the lipid. Similar results were obtained in rats using another inhibitor of fatty-acid oxidation, CVT-4325 [43].

A second possible mechanism supposes that lipid emulsions exert a positive inotropic force, improving the ability of the heart to contract. One study noted that pre-treating

isolated rabbit hearts with ATP prior to administering bupivacaine kept heart contractility and heart rate within 10% of baseline [13]. Another experiment found an increase in contractility and systolic pressure in isolated rat hearts treated with bupivacaine and Intralipid compared to bupivacaine alone [47]. Fettiplace et al conducted trials in which live rats were injected with either a saline solution or Intralipid. The Intralipid group displayed higher aortic flow and blood pressure relative to the saline control group, indicating that the effect of Intralipid on heart contractility cannot be explained as merely a product of an increased volume in the bloodstream [16].

Finally, some have speculated that lipid emulsions restore the voltage potential across myocardial cells, returning ion channels to their normal state. It has been understood for some time that bupivacaine acts by blocking sodium channels, to which the difficulty in toxicity reversal can be ascribed [8]. A study in HEK 293 (Human Embryonic Kidney) cells showed the ability of Intralipid to clear bupivacaine-induced blockage of some sodium channels [39]. Another study performed before the development of ILE therapy determined that long chain fatty acids can modulate the release of calcium in myocardial channels [26]. Building off this foundation, Partownavid et al reported that lipid emulsions increased the amount of calcium required to open the mPTP channel in cardiac mitochondria, an event associated with cell death [43].

In all likelihood, some combination of these factors–the lipid sink, fatty acid metabolism, positive inotropy, and channel regulation–is in play. But if we are not able to describe their relative contributions and interactions, our knowledge of ILE therapy will remain incomplete.

### 1.2.2 Interactions with Vasopressors

Traditional treatment of LAST usually involves injecting the patient with epinephrine, vasopressin, or a combination of the two (vasopressor). These drugs constrict blood vessels, leading to increased blood pressure. In most reports of successful reversal of cardiotoxicty via ILE therapy, the lipid was not given until traditional treatment had been exhausted, meaning that patients likely had epinephrine or vasopressin in their bloodstream. It is fair to ask, therefore, whether there might be an interaction between vasopressors and lipid emulsion, be it negligible, antagonistic, or synergistic. Consensus has not been reached on this matter due to conflicting results and to disagreements over which biological metrics should be weighted most heavily in evaluating recovery.

One subset of researchers holds to the opinion that lipid emulsion should be used in lieu of, and not with, vaspopressors. Weinberg et al induced asystole in rats using bupivacaine infusions of 20 mg/kg and sorted subjects into one of three treatment groups: saline, 30% Intralipid, or epinephrine [51]. They monitored the hemodynamic metrics of rate-pressure product (heart rate times systolic blood pressure), arterial oxygen tension, and central venous oxygen saturation for ten minutes following treatment. Their results concluded that Intralipid promoted superior recovery by the end of the ten minutes. A nearly identical study, differing only in vasopressin being substituted for epinephrine, once again ruled that ILE was the more effective treatment [19]. Some have even pushed to minimize epinephrine use in cases of LAST following research showing that epinephrine may inhibit the ILE mechanism. Hiller et al repeated the conditions of the previous two experiments, but combined 30% Intralipid with increasing doses of epinephrine [22]. Their conclusion was that, though epinephrine may catalyze faster recovery initially, it does not outperform lipid and, furthermore, depresses lipid action above doses of 10

mcg/kg.

These findings, however, have not been overwhelmingly supported by other experiments performed with porcine models. True, some difference in outcome may be attributable to the change in model animal; yet as it will be seen, the results from various porcine studies are hardly uniform in of themselves. Siqueira et al and Mauch et al both conducted studies in which piglets were treated with epinephrine, lipid, or a combination of the two in response to local anesthetic toxicity. The former subjected the piglets to the anesthetic levobupivacaine while the latter utilized bupivacaine [10]. Siqueira observed that the lipid, epinephrine, and lipid/epinephrine treatments, though better than the saline control, were not significantly different in their ability to promote return of spontaneous circulation (ROSC). Conversely, Mauch found that ROSC was only achieved using epinephrine or a combination treatment, but not with lipid alone [36]. Mauch incorporated an additional treatment combining vasopressin and Intralipid, which promoted ROSC at a higher rate than Intralipid alone.

Two other studies conducted in adult pigs, rather than piglets, could not produce strong evidence in favor of ILE therapy over vasopressors. Hicks administered 10 mg/kg of bupivacaine solution to pigs followed by epinephrine and vasopressin [21]. The animals were then split into two treatment groups: one received lipid and the other saline. No significant difference was noted in ROSC. The findings of Mayr were even harsher towards ILE [37]. Pigs were given a dose of 5 mg/kg of bupivacaine solution and provided epinephrine combined with either vasopressin or a 20% lipid emulsion. All pigs in the epinephrine/vasopressin group survived, while none exhibited ROSC in the lipid group.

Consolidating these experiments into a cohesive picture proves a difficult, if not impossible, task. Certainly something can (and has) been said about the use of different animal models and the possibility of high epinephrine concentrations confounding results.

Yet as with postulates on the ILE mechanism, the true answer may yet lie somewhere in the middle. Li et al induced asystole in rats using bupivacaine and treated with either saline, epinephrine, lipid, or lipid combined with varying amounts of epinephrine [33]. They found that lipid combined with small does of epinephrine proved most effective in restoring hemodynamic metrics to baseline. Epinephrine, they hypothesized, encourages bupivacaine and lipid interaction by improving the heart's ability to pump blood. However, no model exists yet to study this potentially cumulative effect.

### 1.2.3 Scope and Safety

ILE Therapy, as discussed previously, has been quickly adapted to treat toxicity events beyond LAST. Some positive results have been reported to this effect, but the practice does not sit well with many clinicians and researchers [7]. A predominant concern is that reporting bias has contributed to the pace at which novel applications have been pursued [50]. For instance, an editorial to Anesthesiology and Intensive Care criticized the use of Intralipid to treat oral overdose of tricyclic antidepressants. The authors chastised "enthusiasts (who) have uncritically extrapolated the use of Intralipid" and accused these enthusiasts of trusting patients' well-being to incomplete science [7].

An incident that fits this profile involved a relatively young individual who was poisoned by cyclic antidepressants [31]. Following unsuccessful resuscitation, ILE therapy was attempted. Of note, the lipid was injected in the femoral area and not in an upper extremity vein as is usually done when treating LAST. The patient was revived following lipid infusion, but she subsequently developed pancreatitis–an inflamed pancreas–and was hospitalized for some time. She eventually made a full recovery, yet the fact that ILE therapy could have led to complications is not trivial.

The previous case was not an isolated one. A survey of two hospitals identified nine

cases in which patients were treated with lipid for events other than LAST [32]. Six of the nine patients experienced complications in the form of either pancretitis or adult respiratory distress syndrome (ARDS). Lab samples from three of the patients were also unreadable because of the high concentration of lipid in the blood, a potentially problematic development were a sample to require immediate analysis. It should be noted that a causality link between ILE therapy and the onset of ARDS has been debated by a study involving parenteral nutrition. Patients already presenting ARDS did indeed experience poorer gas exchange in the lungs relative to the control group after receiving lipid [30]. However, patients who did not already have ARDS showed no decrease in lung function whatsoever. Still, the fact that ILE therapy might exacerbate a pre-existing condition is food for thought.

### 1.2.4 The Need for a Better Model

To label individuals critical of ILE therapy as "opponents" of the practice would be an unfair overstatement. It would be better to say that they are safe practitioners who believe that ILE therapy shows promise but needs further vetting. The question, then, becomes how to further our understanding of ILE Therapy–its mechanism, its interaction with other compounds, and its potential side effects. In the absence of human studies, which are highly unlikely to occur, the most useful information will be gleaned from "models incorporating concurrent investigation into both pharmacokinetic and pharmacodynamic mechanisms of action" [20]. Using a rat model specific to treatment of LAST induced by bupivacaine overdose, this paper seeks to demonstrate how rigorous mathematical and statistical treatment of available data can begin to inform decision-making regarding responsible and successful application of ILE therapy.

## 1.3 Mathematics in Clinical Settings

### 1.3.1 PK/PD Models

Pharmacokinetic (PK) models characterize the concentration and distribution of a drug throughout the body as a function of time [27]. These models can be non-compartmental, in which the body is taken as a whole, but greater detail is achieved by treating the body as a network of connected compartments. Usually, there is a compartment for each organ–though stomach and intestines are frequently lumped as a single unit–as well as the venous and arterial systems. Each compartment is governed by a series of differential equations describing mass conservation of the compound in question. PK models achieve greater power when constructed using previously measured or estimated physiological parameters specific to the subject organism. These physiologically based pharmacokinetic (PBPK) models incorporate "species specific physiological parameters that are independent of the drug...and a drug-specific part which consists of the individual drug's ADME properties" [54]. ADME properties refer to data pertaining to absorption, distribution, metabolism, and excretion [54].

PBPK models are limited in that they do not capture how the changing concentration of a drug effects other physiological processes [12]. That is, they describe "what the body does to the drug", but fail to address "what the drug does to the body" [23]. This shortcoming can be rectified by incorporating a pharmacodynamic component in the model. The underlying principle of pharmacodynamic modeling is that the physiological effect of interest is induced by binding of a drug to associated receptors [27]. Frequently, sigmoid equations of the form

$$E(C) = \frac{E_{max}C^n}{EC_{50}^n + C^n} \tag{1}$$

are used to characterize the concentration ($C$)-dependent effect ($E$) of the drug [27]. The additional parameters in Equation 1 are the maximum possible effect of the drug ($E_{max}$), the drug concentration at which half the maximum effect is achieved ($EC_{50}$), and a fitting parameter $n$. Note that an equation of this form implies that at high drug concentrations the receptor in question will become saturated [27]. The drug concentrations supplied to Equation 1 are obtained via pharmacokinetic relationships, creating a physiologically based pharmacokinetic/pharmacodynamic (PK/PD) model.

### 1.3.2 A PK/PD Model for ILE Therapy

The model which shall be used in this study is a compartmental, physiologically based PK/PD model specific to ILE treatment of LAST caused by intravenous overdose of bupivacaine. The differential equations governing dispersal of bupivacaine throughout the compartments illustrated in Figure 1 are detailed by Kuo and Akpa [29], the developers of the model. Underlying the pharmacokinetics of the model are the assumptions that bupivacaine is hepatically cleared and rate-perfusion limited [29]. The latter consideration, generally applied for small lipophillic molecules like bupivacaine, presumes that the limiting factor in absorption is blood flow to tissue [54]. Furthermore, bupivacaine is assumed to be partitioned between bound and unbound (i.e. free in the plasma) states [29]. Four possible binding sites are considered: red blood cells, lipid, and the blood proteins human serum albumin (HSA) and $\alpha - 1$ acid glycoprotein (AAG) [29]. The mathematical relationships governing equilibrium between these binding states are described in detail by Kua and Akpa. Meanwhile, metabolism of the lipid in all com-

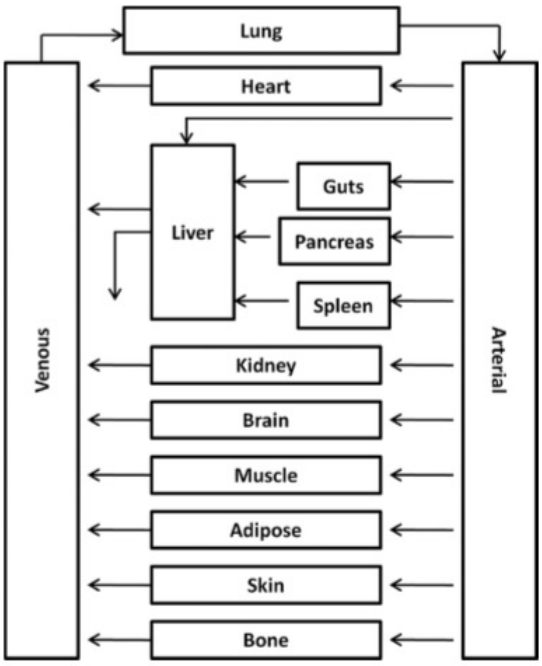


Figure 1: Physiologically Based Compartmental Pharmacokinetic Model for Bupivacaine [29]

partments is described by a Michelis-Menten expression [14], which is a Hill function (Equation 1) with the tuning parameter set at $n = 1$.

The pharmacodynamics constructed upon this PK scaffold account for the effects of the bupivacaine and lipid concentrations on cardiac output. More detail will be provided on these equations, as documented by Fettiplace et al, because the parameters of interest to this study are contained therein. The action of bupivacaine is assumed to be a Hill function of the form [14]

$$E_{bup} = \frac{C^{\beta}_{bup,tis}}{EC^{\beta}_{50,bup} + C^{\beta}_{bup,tis}}. \tag{2}$$

Note that the bupivcaince concentration of interest ($C_{bup,tis}$) is specifically that in the cardiac tissue (tis).

Lipid dynamics are apportioned between two equations. The first describes the po-

tential inotropic effect of lipid [14].

$$E_{lipid} = \frac{E_{max,lip} C_{lip,plasma}^{n}}{EC_{50}^{n} + C_{lip,plasma}^{n}}. \tag{3}$$

Unlike Equation 2, the concentration of interest in Equation 3 is that of the lipid in the blood plasma. The parameters $E_{max,lip}$ and $EC_{50}$ account for the maximal lipid effect and the concentration at which half the maximum effect is achieved, respectively. Once again, $n$ is a Hill-type fitting parameter. The other equation specifying lipid dynamics allows for a change in cardiac output resulting from the increased volume in the bloodstream caused by lipid infusion [14].

$$E_{vol} = K_{volume}(\frac{Q_v}{Q_b} - 1). \tag{4}$$

$K_{volume}$ is a proportionality constant, while the ratio of $Q_v$ to $Q_b$ is that of the return veinous blood flow rate to the baseline rate.

Finally, cardiovascular response to these factors ($E_{bup}$, $E_{lip}$, and $E_{vol}$) is modeled via the two relationships below [14]:

$$\frac{dU}{dt} = \begin{cases} k_p(Q_{co} - Q_b) & Q_{co} > Q_b \\ -k_p U & Q_{co} \leq Q_b \end{cases} \tag{5a}$$

$$Q_{co} = Q_b(1 - E_{bup})(1 + E_{lip})(1 + E_{vol})(1 - \alpha U). \tag{5b}$$

The variable $U$ captures the action of homeostasis, regulated in Equation 5a via proportional feedback control. $Q_{co}$ and $Q_b$ represent the time-dependent cardiac output and the baseline cardiac output, respectively.

Equation 5b represents an interesting opportunity for a novel addition to this PK/PD

model. As it is written, there is an implicit assumption that the relative weights of the volume, lipid, and bupivacaine terms remain unchanged across the treatment interval. However, recent research performed by Fettiplace et al suggests that the high bupivacaine concentration in the cardiac tissue initially damps the inotropic and metabolic benefits of ILE [15]. Only once a sufficient amount of the drug has been "scavenged" by the lipid, to borrow their term, can the positive effects of inotropy and lipid metabolism be realized [15]. Thus, the parameters in Equations 5a and 5b (and, by extension, Equations 2-4) may exhibit a time dependence that cannot be captured by the model as is.

### 1.3.3 Personalized Medicine and Virtual Populations

As with all developing PK/PD models, preliminary studies with the model just described have relied upon parameter values averaged over a population. However, individual differences in response to both bupivacaine and lipid infusion may significantly impact predictions made by the model. This possibility touches upon what has become a prevalent theme in emerging medical research: personalized medicine. This notion asserts that patient wellness can be improved by considering individual genotypic and phenotypic biomarkers in both diagnosis and treatment [24]. In the case of ILE therapy, such biomarkers could include any one of the parameters in Equations 2–4.

Somewhat paradoxically, these individual parameters can also inform our expectation of a population-level response. This is accomplished by fitting an appropriate distribution to the individual parameters, randomly sampling from it, and simulating an expected response using mathematical modeling to create a virtual individual [42]. By repeating this process, a virtual population can be constructed from which a feasible range of expected outcomes can be inferred.

## 1.4 Goals of this Paper

Given all that has been presented, the goal of this paper is threefold. First, we will explore the impact of introducing time dependency to subsets of model parameters. We hope that this will both improve model accuracy and provide insight as to the relative roles of the various mechanisms of ILE action that have been postulated. Furthermore, we will estimate both time dependent and constant model parameters on an individual level, allowing us to approximate their distributions. We will then use these distributions to construct a virtual population characterizing the response of rats to ILE treatment of LAST induced by bupivacaine. In doing so, we seek to illustrate how one might use individual bio-markers to identify candidates who would most benefit from ILE therapy.

# 2 Parameter Estimation 1

## 2.1 Data and Methods

### 2.1.1 Data

The data used for this analysis originated in a study performed by Fettiplace et al [16] investigating the effect of lipid infusion on cardiac function in rats. Animals were administered either saline ($N = 6$) or 20% Intralipid ($N = 7$) at a rate of 9 mL/kg/min for 1 minute and their relative blood flow rates (among other metrics) were monitored. The data ranges from time $t = 0$ minutes to $t = 9$, downsampled to 540 data points (1 per second). Since only lipid, and not bupivacaine, was given, the pharmacodynamic parameters that can potentially be estimated from the data set are those in Equations 3 and 4, summarized in Table 1. Physiological parameters relevant to the PK aspect of

the model are taken to be those of a 400 g male Sprauge-Daley rat as calculated using per unit mass values from [29].

Table 1: Candidate Parameters for Estimation in Individual Rat Response to ILE Infusion

| Parameter | Description |
|---|---|
| $E_{lip,max}$ | Maximum inotropic effect of lipid (Equation 3) |
| $EC_{50}$ | Lipid concentration at which half of maximum inotropic effect is achieved (Equation 3) |
| $n$ | Fitting parameter describing inotropic effect of lipid (Equation 3) |
| $K_{volume}$ | Flow promoting effect of additional volume in heart (Equation 4) |
| $\alpha$ | Tuning parameter for homeostatic response (Equations 5a, 5b |
| $k_p$ | Proportional control constant for homeostasis response (Equations 5a, 5b) |

### 2.1.2 Cardiac Function Adjustment

The PK/PD model used for this study was identical to that developed in [29] and [14] save for one alteration. A modified representation of the homeostatic response (Equations 5a and 5b), was implemented via

$$\frac{dU}{dt} = k_p(Q_{co} - Q_b) \tag{6a}$$

$$Q_{co} = \begin{cases} Q_b(1 - E_{bup})(1 + E_{lip})(1 + E_{vol})(1 - \alpha U) & Q_{co} \geq Q_b \\ Q_b(1 - E_{bup})(1 + E_{lip})(1 + E_{vol})(1 - \dfrac{\alpha U}{|Q_b - Q_{co}| + 1}) & Q_{co} < Q_b. \end{cases} \tag{6b}$$

As before, $Q_{co}$ is the cardiac output at time $t$ and $Q_b$ is the baseline cardiac output. This

change was introduced because the numerical differential equation solver used for this study (*ode15s.m* in MATLAB) requires that solutions be continuously differentiable on their domain. However, a discontinuity is produced in Equation 5a when $Q_{co}$ approaches $Q_b$ from above. Thus, the conditional aspect of the homeostatic model was transferred to the equation specifying cardiac output. Note that this was done in such a way as to ensure continuity in Equation 6b when $Q_{co} = Q_b$. While the optimal values of $\alpha$ and $k_p$ characterizing Equation 6b will differ from those that accomplish likewise for Equation 5b, the behavior originally intended by [14] will be preserved. This fact was verified over the course of our study.

### 2.1.3 Inverse Problems

The task of inferring parameter values from data is classified as an inverse problem. Suppose we have a mathematical model of the form [48]

$$\begin{aligned} \frac{dy}{dt} &= g(t, y(t), Q) \\ y(t_0) &= y_0. \end{aligned} \tag{7}$$

This model describes a vector of state variables, $y$, whose derivative is a function of $y$, time, and a parameter set $q$. In our case, $y$ is 43-dimensional, comprised of the bupivacaine concentration, lipid concentration, and total volume in each of the fourteen organ compartments, as well as Equation 6a. The parameter set $Q$ consists of physiological parameters (i.e. flow rates, organ volumes, partition coefficients, etc.), which we will assume to be known, and the the parameters in Table 1 (with, where appropriate, their spline representations), which we assume are unknown. We will denote the unknown parameter subset as $\theta$. Suppose also that we have a process that relates $y$ to an observable

state at discrete time points. That is, we have

$$f(t_i, \theta_0) = h(y(t_i), \theta_0), \qquad i = 1, ..., N. \tag{8}$$

The observable function for this PK/PD model is Equation 6b, which maps the state vector and parameters of interest to the cardiac output at each of the $N = 540$ sample points. Since we cannot assume perfect measurement of the cardiac outputs recorded by [16], we utilize a statistical model of the form

$$Y_i = f(t_i, \theta) + \mathcal{E}_i. \tag{9}$$

The random variable $\mathcal{E}_i$ represents measurement error, which causes discrepancy between the random variable for the perceived observable state ($Y_i$) and the actual observable state ($f(t_i, \theta)$). We assume that the errors are independently and identically distributed (i.i.d) with mean $\bar{\mathcal{E}} = 0$. Realizations of the data correspond to realizations of the random variables $Y_i$ and $\mathcal{E}_i$ such that

$$y_i = f(t_i, \hat{\theta}) + \epsilon_i, \tag{10}$$

where $\hat{\theta}$ is a parameter set estimating the true parameter set $\theta_0$. We obtain $\hat{\theta}$ by minimizing the ordinary least squares (OLS) cost [48]

$$S(y_i, \theta) = \sum_{i=0}^{N} [y_i - f(t_i, \theta)]^2. \tag{11}$$

The set $\hat{\theta}$ offering the best approximation of $\theta_0$, which lies in the admissable parameter space $Q$, is thus [48]

$$\hat{\theta} = argmin_{\theta \in Q} \sum_{i=0}^{N} [Y_i - f(t_i, \theta)]^2. \tag{12}$$

An unbiased estimate of the observation variance associated with the estimated vector $\hat{\theta}$, assuming $r$ data points and $p$ parameters, is [48]

$$\hat{\sigma}_0^2 \approx \frac{1}{r-p} \sum_{i=1}^{n} [y_i - f(t_i, \hat{\theta})]^2. \tag{13}$$

Since $f(t_i, \theta)$ is a function of a system of differential equations, we require numerical integration software to solve Equation 12. We apply the Matlab function *ode15s.m*–a stiff differential equation solver–for this purpose.

Solutions to Equation 12 are generated in two steps. First, in order to avoid becoming trapped in a local minimum neighboring the literature average values of our parameters of interest (used as our initial estimates), we perform a Direct search global optimization. In short, Direct search operates by transforming the problem domain into an N-dimensional hyper-cube with side length equal to one [17]. The algorithm first determines $f(c_1)$, which is the cost function (Equation 11, in this case) evaluated at the center of the cube. Next, the costs $f(c_1 \pm \delta e_i)$ are calculated, where $\delta$ is one-third the length of the cube side and $e_i$ is the unit vector in the $ith$ direction. Direct search then establishes a weight along each direction [17]

$$w_i = min(f(c_1 + \delta e_i), f(c_1 - \delta e_i)), \quad 1 \leq i \leq N. \tag{14}$$

The region with the minimum $w_i$ is divided into thirds. Direct search then identifies "potentially optimal" regions, divides them as in the initiation step along the longest dimension, and calculates the corresponding weights $w_i$ [17]. This process is repeated until a global minimum is found as determined by a pre-established tolerance level.

We further refine the parameter estimates obtained through the Direct search by introducing them as initial estimates to the Matlab non-linear least squares solver *lsqnonlin.m*.

This function operates using a trust region reflective least squares algorithm, described in great detail by Coleman and Li [9]. It should be noted that, due to the large range in magnitudes of the parameter values reported by Fettiplace et al [14], all optimization steps are performed using log-transformed parameters.

### 2.1.4 Uncertainty Quantification and Subset Selection

We seek to determine which of the parameters from Table 1 can be reliably estimated from the data. Reliability, in this context, requires keeping the parameter standard errors low. To quantify these errors, we estimate all six candidate parameters for each rat. We then construct a sensitivity matrix, $\chi$, composed of elements

$$\chi_{i,j} = \frac{\partial Y(t_i, \hat{\theta})}{\partial \hat{\theta}_j}. \tag{15}$$

That is, the entry in the $ith$ row and $jth$ column is the partial derivative of the model output (a function of a vector of estimated parameters $\hat{\theta}$, as before) with respect to the $jth$ parameter at the $ith$ time step [4]. The sensitivity matrix must usually be estimated numerically, and we elect to do so using the complex step method. This method makes use of the relationship [4]

$$\frac{\partial f}{\partial x} = lim_{h \to 0} \frac{Im[f(x + ih)]}{h}. \tag{16}$$

The operator $Im$ represents the imaginary component of the specified value. When $h$ is extremely small (i.e. to machine precision), we can make the approximation [4]

$$\frac{\partial f}{\partial x} \approx \frac{Im[f(x + ih)]}{h}. \tag{17}$$

Once the sensitivity matrix is obtained, we construct a covariance matrix [48]

$$\hat{\Sigma} = \hat{\sigma}_0^2[\chi(\hat{\theta})^T \chi(\hat{\theta})]^{-1}. \tag{18}$$

The model variance $\hat{\sigma}_0^2$ is obtained from Equation 13. We obtain an estimate of the standard error of the $kth$ parameter from the main diagonal of the covariance matrix $\hat{\Sigma}$ according to [48].

$$SE(\hat{\theta}_k) = \sqrt{\hat{\Sigma}_{kk}}. \tag{19}$$

It is possible that we can drive up parameter standard errors by attempting to fit too many parameters. To avoid this pitfall, we solve the inverse problem assuming estimation of all parameters and construct $\chi$. We then take a subset of parameters and construct a new covariance matrix, $\hat{\Sigma}'$ by taking the columns from $\chi$ that correspond to the chosen parameters and solving Equation 18. We obtain the parameter standard errors for the subset by applying Equation 19 to $\hat{\Sigma}'$. These standard errors describe a problem in which the chosen subset is estimated and the other parameters are left constant. We divide the standard errors by the associated parameter values to obtain normalized standard errors and compare them to the value $\frac{1}{1.96}$. A standard error below this value guarantees that the lower bound of a 95% confidence interval for the associated parameter will be positive. We repeat this process for every possible parameter subset and choose the combination that yields the greatest number of parameters with normalized standard errors below the $\frac{1}{1.96}$ boundary. For this study, there were $\sum_{n=1}^{6} \binom{6}{n} = 64$ possible parameter subsets.

### 2.1.5 Time Varying Parameters

We approximate temporal variation in the selected parameters by treating them as piece-wise, continuous functions of time. That is, we describe a time-varying parameter $P(t)$

using $m$ linear functions as [44]

$$P(t) = \begin{cases} p_1(t) = a_1 + b_1 t & t \in [t_0, t_1) \\ p_2(t) = a_2 + b_2 t & t \in [t_1, t_2) \\ \vdots & \\ p_m(t) = a_n + b_1 t & t \in [t_{m-1}, t_m] \end{cases} . \tag{20}$$

The times $t_1, t_2, ..., t_{m-1}$ are the times at which the function changes behavior. By enforcing continuity at these transitions (i.e. $p_1(t_1) = p_2(t_1)$, $p_2(t_2) = p_3(t_2)$, etc), we create a spline function. The endpoints of the splines are referred to as nodes, of which there are $m+1$. Two nodes are external, at $p_1(t_0)$ and $p_m(t_m)$, while $m-1$ nodes occur internally at $p_1(t_1)...p_{n-1}(t_{n-1})$. Spline functions need not be constructed of linear functions, nor are the nodes required to be evenly spaced across the time domain. However, given the size of our model, it was computationally sensible to treat them as such.

Representation of a spline function in Matlab can be accomplished by creating $m+1$ variables corresponding to the function value at each node location. When specified with a vector of times $[t_0, t_1, \ldots, t_m]$, the function *interp1.m* performs linear interpolation between the appropriate nodes as dictated by the input time. Spline functions representing the parameters identified by subset selection are incorporated in the model. Optimization requires estimation of the node locations, growing the parameter set by $pm$ (where $p$ is the number of parameters selected for time variation). To characterize the trade-off between model performance and computational efficiency, we investigate spline approximations of $m = 1$, $m = 4$, and $m = 8$ in the time-varying models. We select these values so that splines can be progressively nested each time $m$ is increased, allowing us to perform model comparison nested restraint tests.

### 2.1.6 Model Selection

Model selection seeks to extract from a candidate pool a single model that provides the best fit to the data while avoiding unnecessary complexity and overfitting. Referred to as the "Principle of Parsimony", this balance is determined by the number of parameters estimated [25]. Too few parameters will result in a biased model, while too many will drive up the variance and make the model unreliable for out-of-sample predictive purposes. One method of quantifying the appropriateness of a model is to apply the Akaike Information Criterion [48]

$$AIC = rln(\frac{S_{min}}{r}) + r(1 + ln(2\pi)) + 2(p + 1). \tag{21}$$

The variables $r$ and $p$ refer to the number of sample points and the number of parameters in the model, respectively. $S_{min}$ is the minimum value of Equation 11 achieved by applying the parameters satisfying Equation 12. Models with lower AIC scores are considered to be the most appropriate for the data in question.

A drawback to relying solely upon AIC is that the difference between two scores does not directly translate to a statement of statistical significance. We therefore supplement our model selection procedure with model comparison nested restraint tests. Nested restraint tests assume two models with parameter estimates $\hat{\theta}$ and $\hat{\theta}_N$ belonging to respective admissible spaces $Q$ and $Q_N$, with $Q_N \subset Q$ [48]. That is, the estimates in $\hat{\theta}_N$ are a subset of the estimates in $\hat{\theta}$. We desire to know whether the true parameter $\theta_0$ is in the subset $Q_H$; therefore we test the null hypothesis $H_0 : \theta_0 \in Q_N$, against the alternative $H_A : \theta_0 \in Q$ [48]. If we denote $S_{min}$ and $S_{min}^{(N)}$ as the minimum OLS costs corresponding to $\hat{\theta}$ and $\hat{\theta}_N$ (solutions of Equation 12), then clearly $S_{min} \leq S_{min}^{(N)}$ because $\hat{\theta}$ contains at least as many parameter values as $\hat{\theta}_N$. Allowing $r$ to be the number of sample data

points, we can thus define a test statistic [48]

$$T = \frac{r(S_{min}^{(N)} - S_{min})}{S_{min}}. \tag{22}$$

The statistic $T$ can be compared to a $\chi^2$ distribution with degrees of freedom equal to the difference in the number of parameters contained in $\hat{\theta}$ and $\hat{\theta}_N$. These tests will be utilized in conjunction with AIC scores to determine which parameters identified by subset selection should be treated as time varying and to establish the number of splines sufficient to represent them.

## 2.2 Results

The results of subset selection for one of the subjects are presented in Figure 2. We note that, across all subjects, the consistent consensus was that $n$ and one of the control parameters (either $\alpha$ or $k_p$) should be estimated. Since analysis of the off-diagonal entries of the covariance matrices demonstrated $\alpha$ and $k_p$ to be perfectly correlated, the choice between the two was inconsequential and we arbitrarily selected $\alpha$. Spline representations of $n$ and $\alpha$ were thus incorporated in the PK/PD model for estimation and the remaining parameters in Table 1 were set to their population averages and not estimated. We hereafter refer to our candidate models as Constant, $mn$, $m\alpha$, and $mn/\alpha$, where $m$ represents the number of splines used to describe time variance (either 1, 4, or 8) and $n$, $\alpha$, and $n/\alpha$ denote which parameters are selected for time variance.

The corresponding model fits for m = 0, 1, 4, and 8 splines are presented in Figures 3-9, in which both $n$ and $\alpha$ are assumed to be time variant. We should note that the number of splines used for $n$ and $\alpha$ are always equal (that is, for instance, there is no model where $n$ is represented by four splines while $\alpha$ incorporates eight splines). In all

cases, a simulated dose of 9 mL/kg of Intralipid is injected at a constant rate for 1 minute starting at time $t = 0$. We then compare the one, four, and eight spline functions for $n$ and $\alpha$ across all subjects to establish potential population trends (Figures 10-11).

Akaike Information Criterion (AIC) scores are tracked across all parameter and spline combinations for each subject in Figures 12-13. Figure 14 summarizes how growing the number of splines affects AIC scores of all subjects with respect to the model in which $n$ and $\alpha$ both vary (which was clearly superior to the other models). Finally, we present the distributions of $n$ and $\alpha$ at each node location for the four spline model (Figure 15) to motivate our choice of probability function from which to sample for our virtual population study.

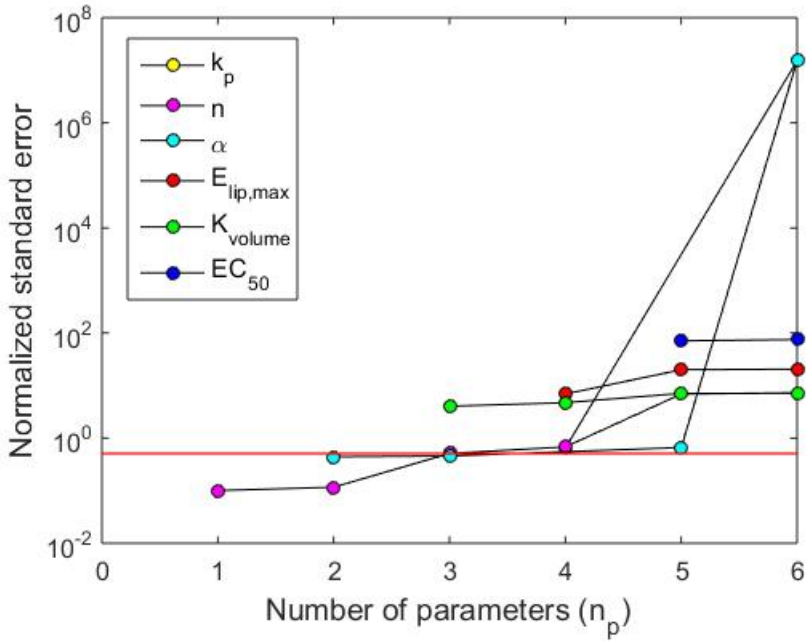


Figure 2: Subset selection results for candidate parameters for estimation. Red line denotes a normalized standard error less than $\frac{1}{1.96}$. The colored circles indicate the combination of $n_p$ parameters that produce the lowest error. These results indicate that no more than two parameters can be estimated with reasonable confidence from the available data. The identities of these parameters are $n$ and $\alpha$. Results are with respect to Subject 5 but are typical of all subjects

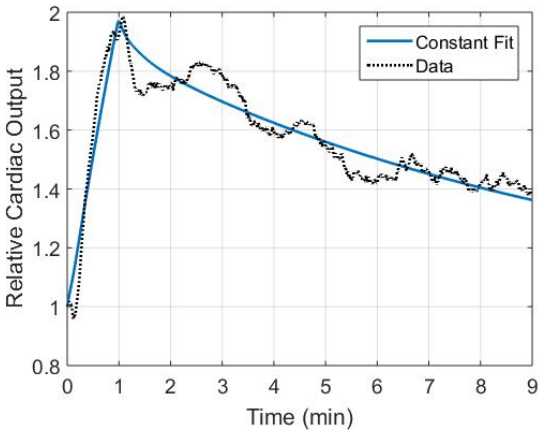


(a) Rat 1: Constant estimates

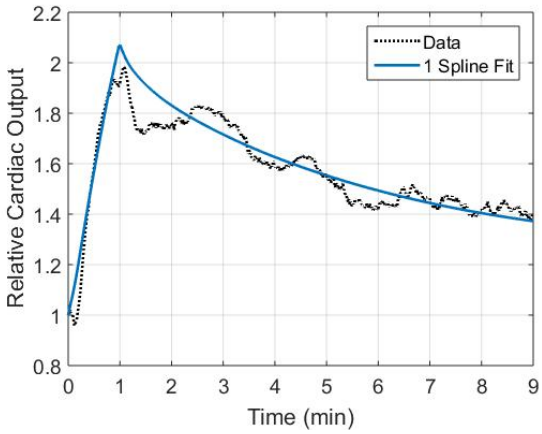


(b) Rat 1: One spline estimates

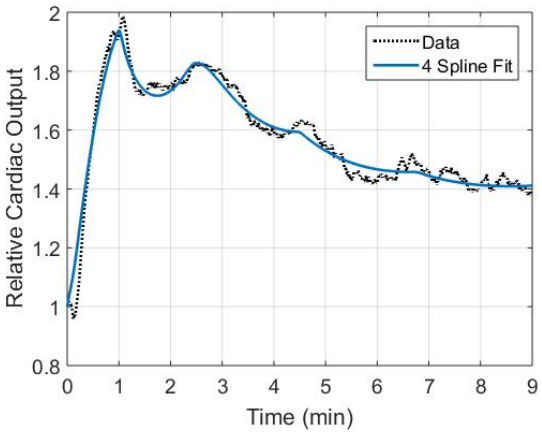


(c) Rat 1: Four spline estimates

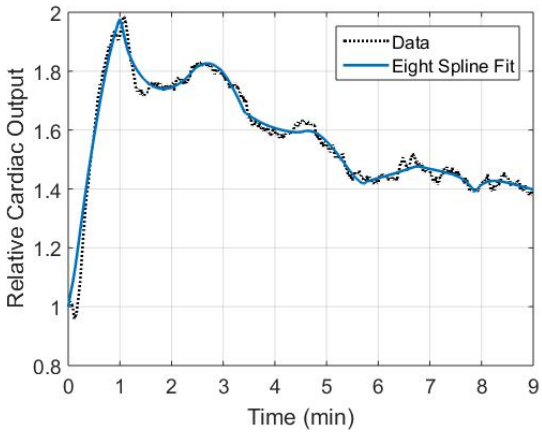


(d) Rat 1: Eight spline estimates

Figure 3: Predicted cardiac output for rat 1 estimating $n$ and $\alpha$ as (a) constant parameters and as time varying parameters via (b), one, (c) four, and (d) eight linear splines

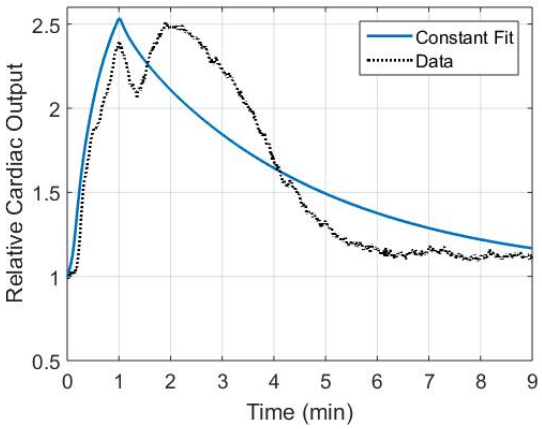


(a) Rat 2: Constant estimates

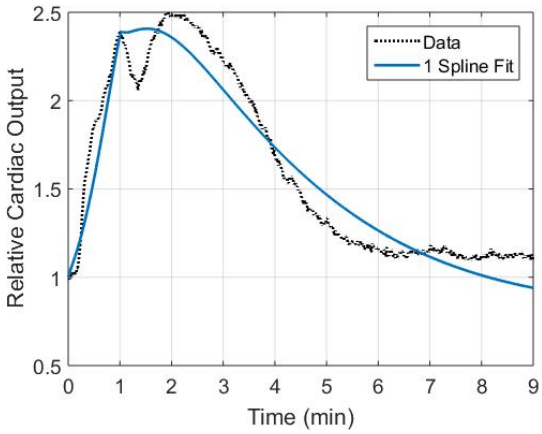


(b) Rat 2: One spline estimates

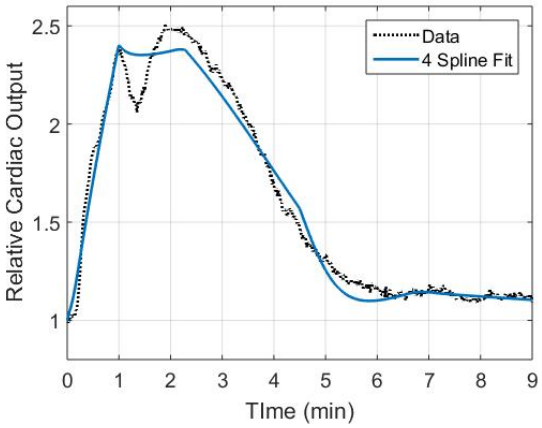


(c) Rat 2: Four spline estimates

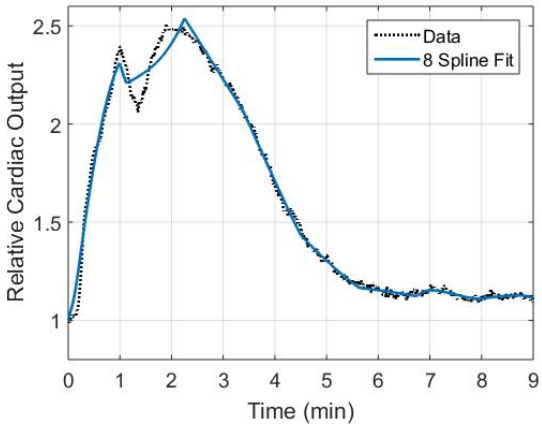


(d) Rat 2: Eight spline estimates

Figure 4: Predicted cardiac output for rat 2 estimating $n$ and $\alpha$ as (a) constant parameters and as time varying parameters via (b), one, (c) four, and (d) eight linear splines

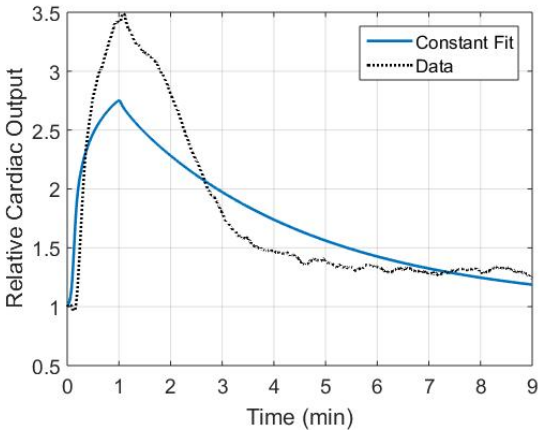


(a) Rat 3: Constant estimates

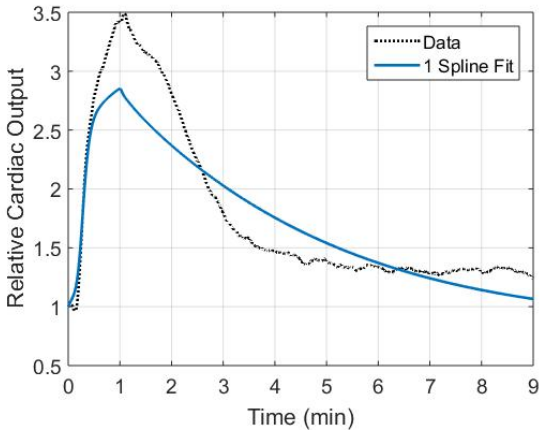


(b) Rat 3: One spline estimates

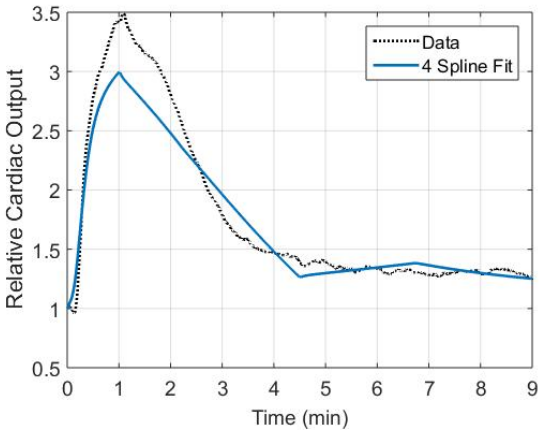


(c) Rat 3: Four spline estimates

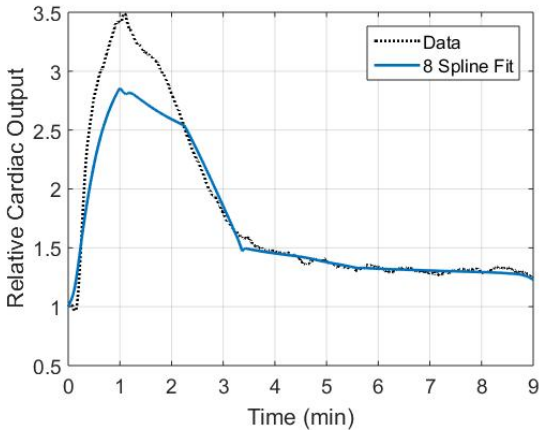


(d) Rat 3: Eight spline estimates

Figure 5: Predicted cardiac output for rat 3 estimating $n$ and $\alpha$ as (a) constant parameters and as time varying parameters via (b), one, (c) four, and (d) eight linear splines

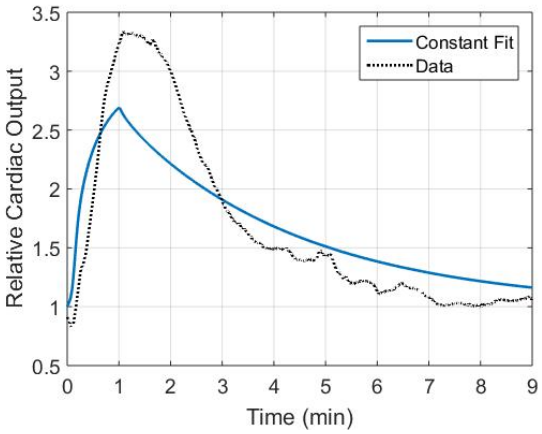


(a) Rat 4: Constant estimates

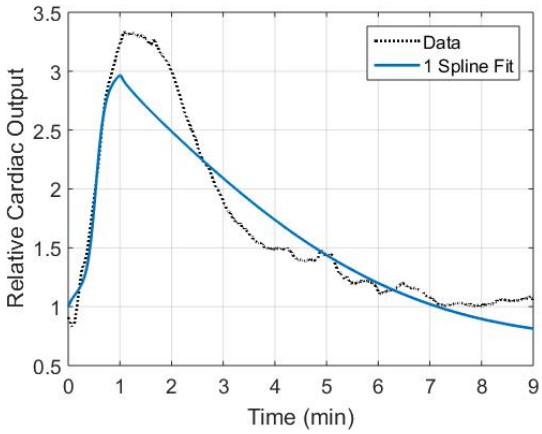


(b) Rat 4: One spline estimates

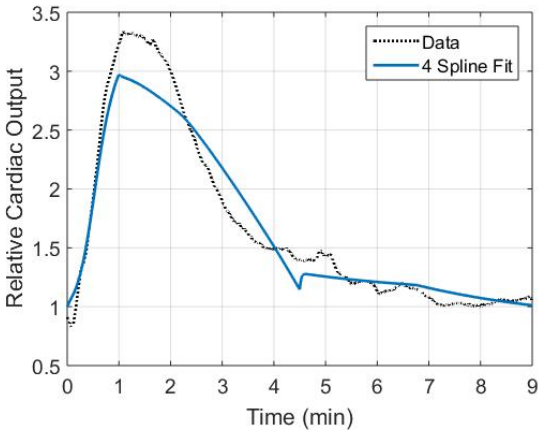


(c) Rat 4: Four spline estimates

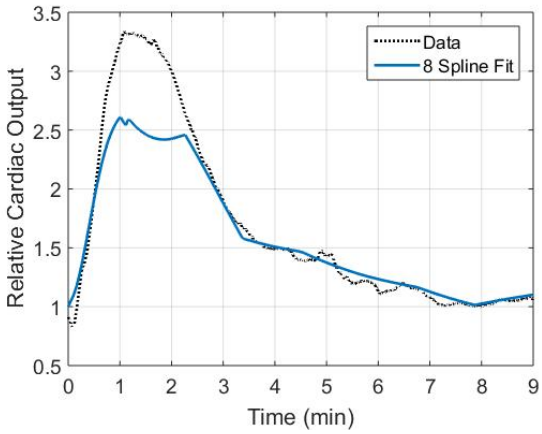


(d) Rat 4: Eight spline estimates

Figure 6: Predicted cardiac output for rat 4 estimating $n$ and $\alpha$ as (a) constant parameters and as time varying parameters via (b), one, (c) four, and (d) eight linear splines

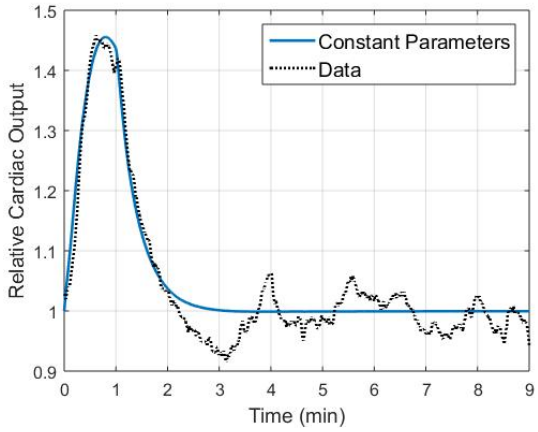


(a) Rat 5: Constant estimates

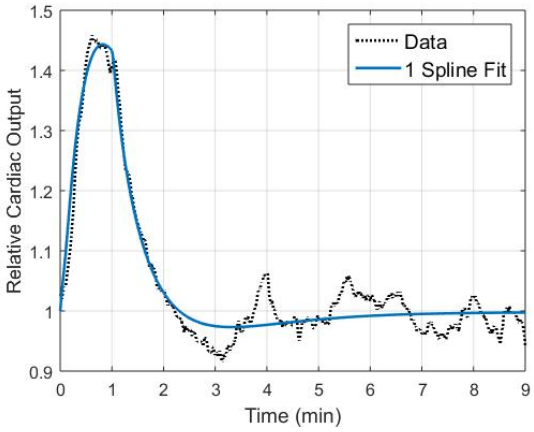


(b) Rat 5: One spline estimates

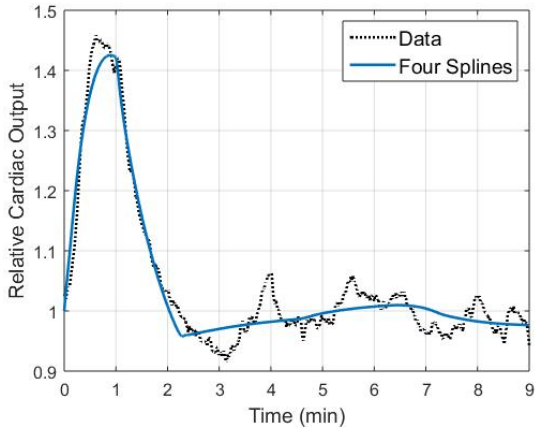


(c) Rat 5: Four spline estimates

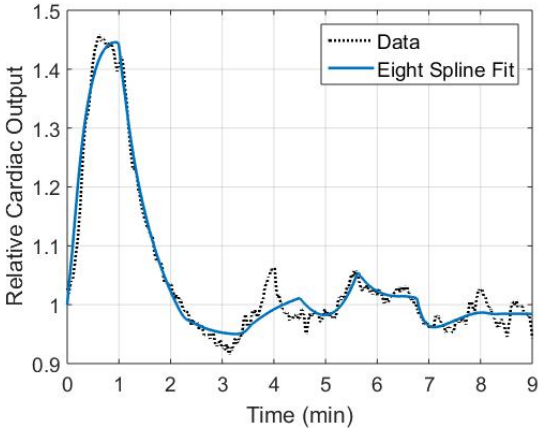


(d) Rat 5: Eight spline estimates

Figure 7: Predicted cardiac output for rat 5 estimating $n$ and $\alpha$ as (a) constant parameters and as time varying parameters via (b), one, (c) four, and (d) eight linear splines

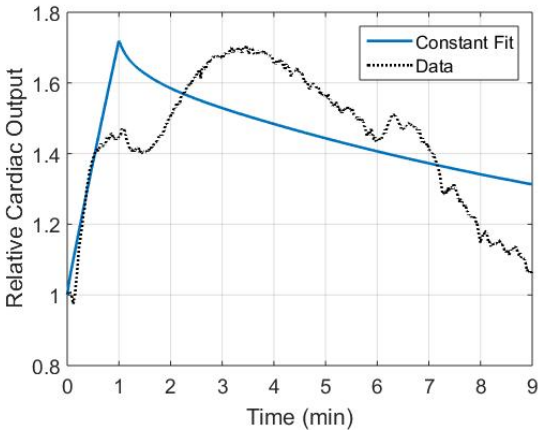


(a) Rat 6: Constant estimates

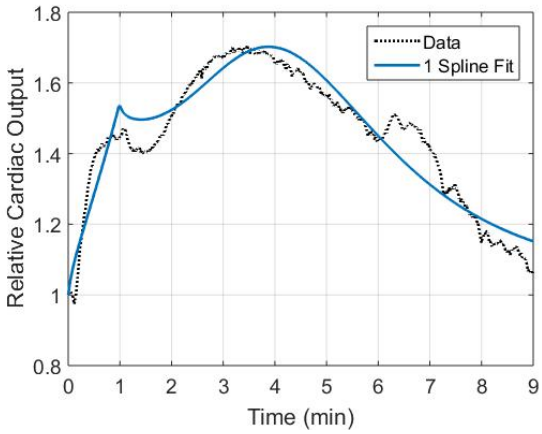


(b) Rat 6: One spline estimates

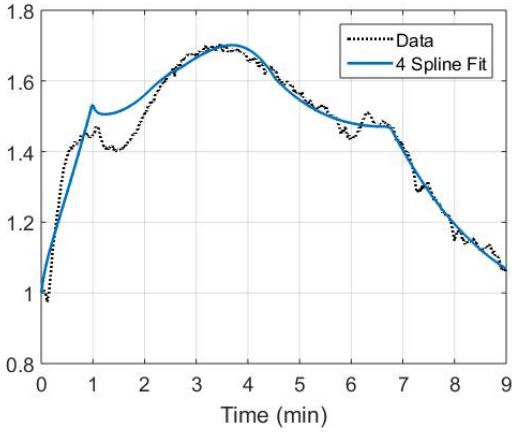


(c) Rat 6: Four spline estimates

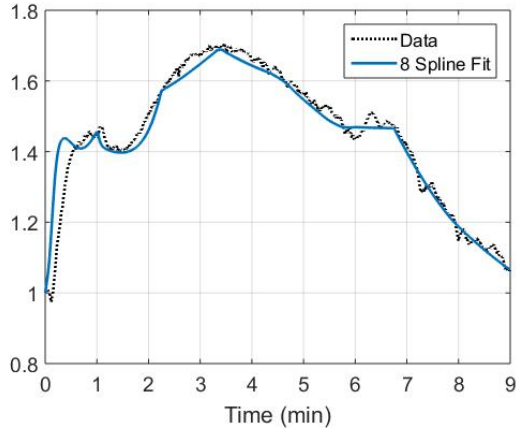


(d) Rat 6: Eight spline estimates

Figure 8: Predicted cardiac output for rat 6 estimating $n$ and $\alpha$ as (a) constant parameters and as time varying parameters via (b), one, (c) four, and (d) eight linear splines

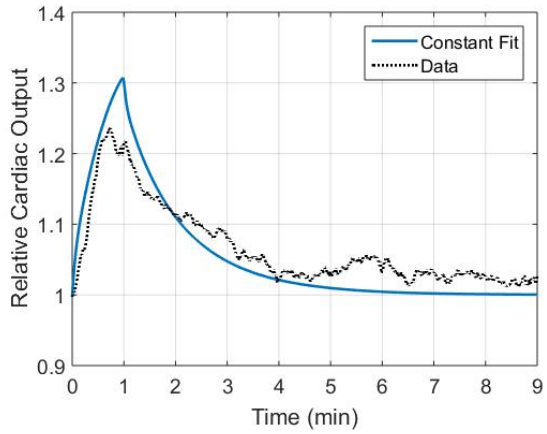


(a) Rat 7: Constant estimates

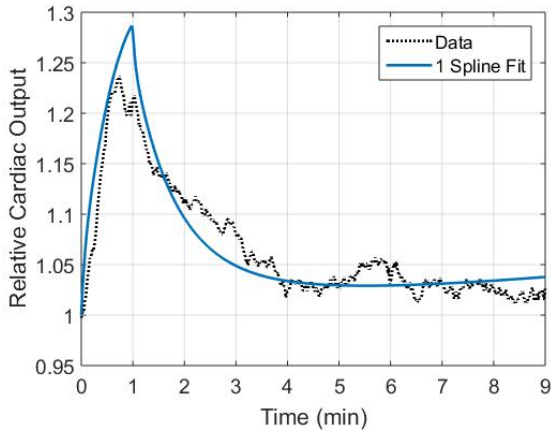


(b) Rat 7: One spline estimates

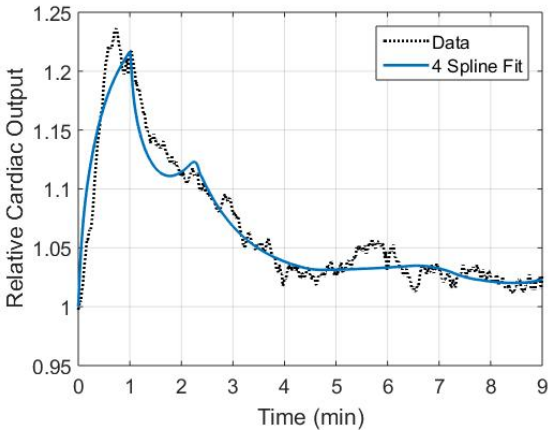


(c) Rat 7: Four spline estimates

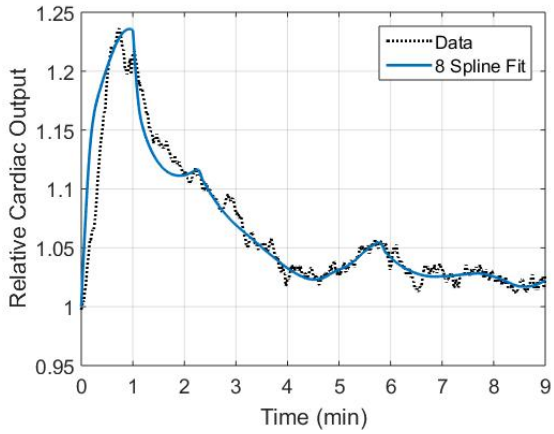


(d) Rat 7: Eight spline estimates

Figure 9: Predicted cardiac output for rat 7 estimating $n$ and $\alpha$ as (a) constant parameters and as time varying parameters via (b), one, (c) four, and (d) eight linear splines

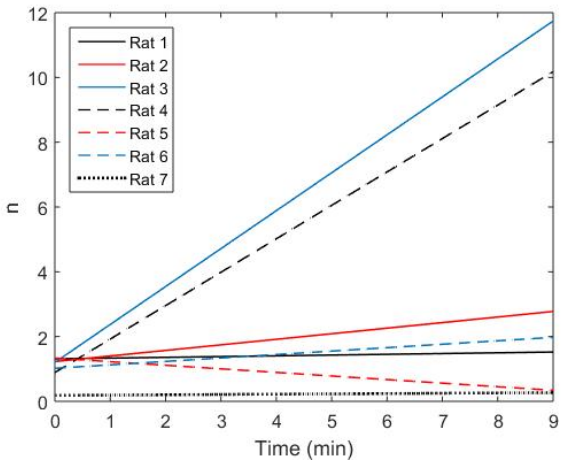


(a) m = 1

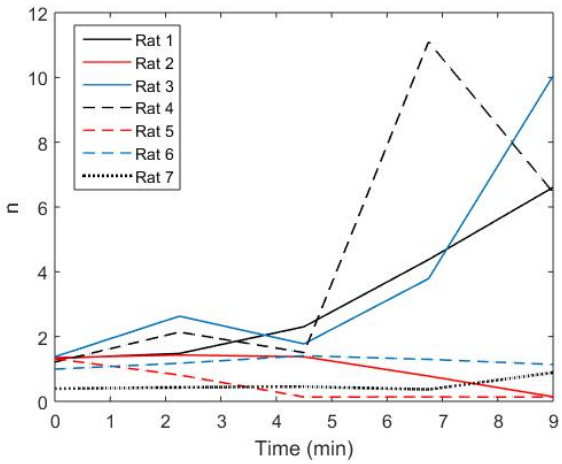


(b) m = 4

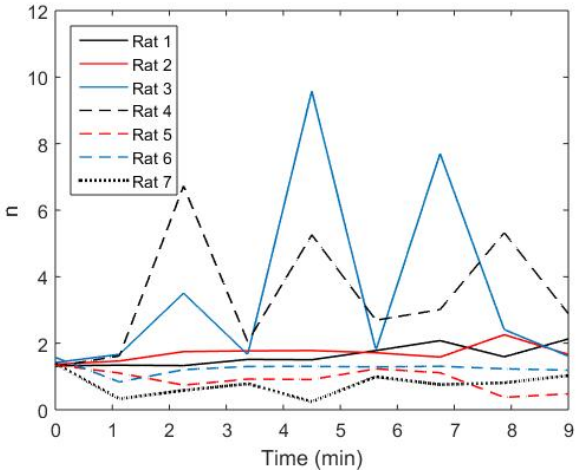


(c) m = 8

Figure 10: Comparison of spline representations for the parameter $n$ using (a) m = 1 spline, (b) m = 4 splines, and (c) m = 8 splines

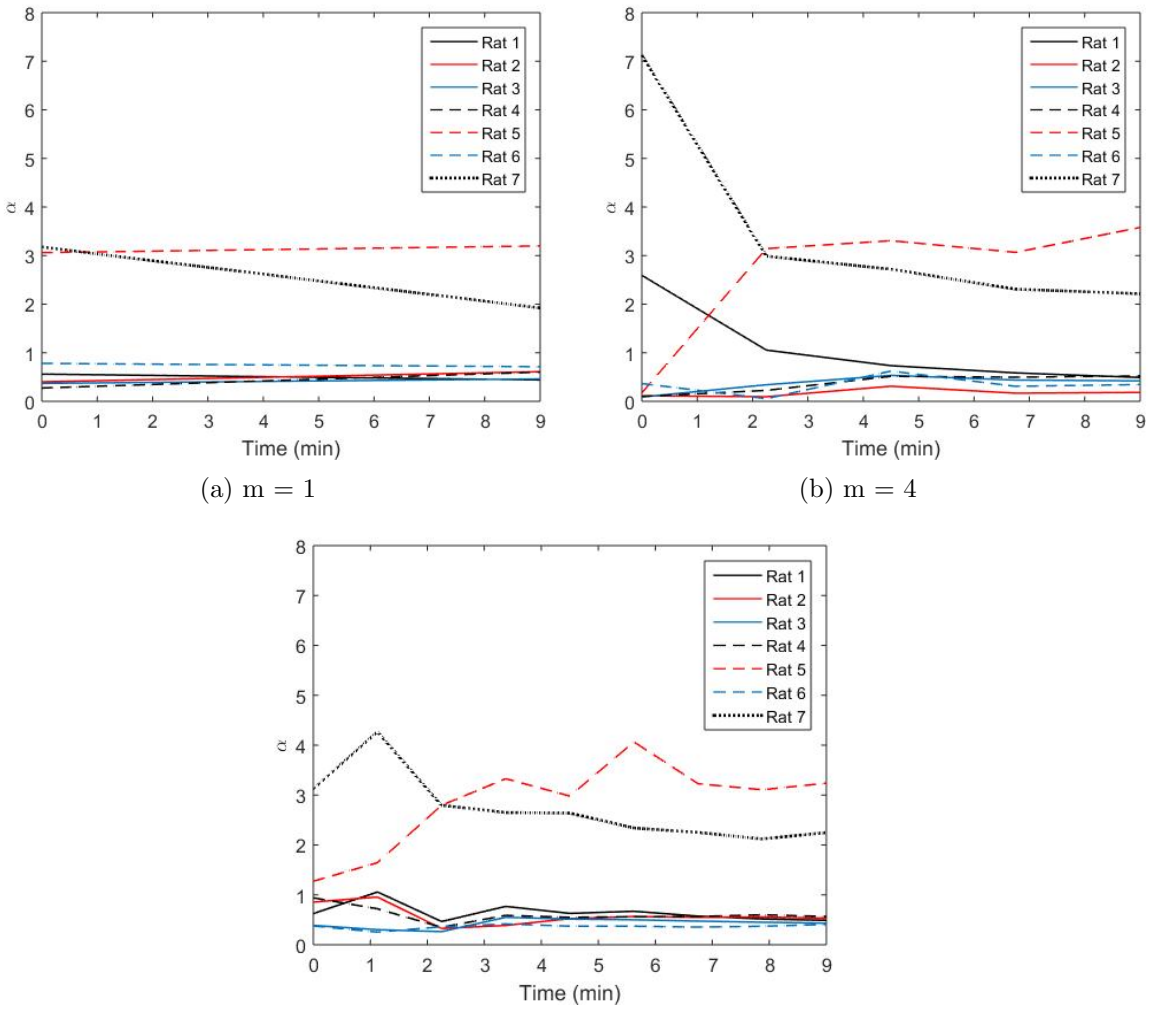


(a) m = 1

(b) m = 4

(c) m = 8

Figure 11: Comparison of spline representations for the parameter $\alpha$ using (a) m = 1, (b) m = 4 splines, and (c) m = 8 splines

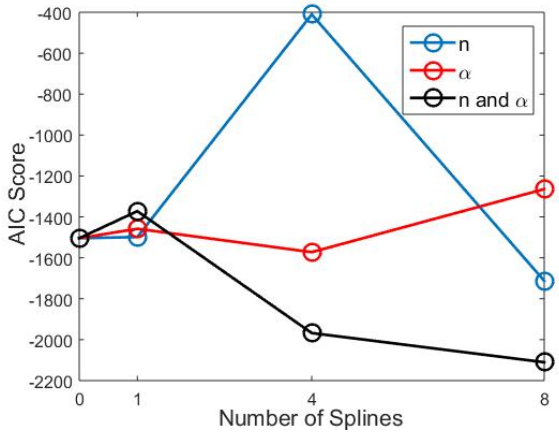


(a) Rat 1: AIC Scores

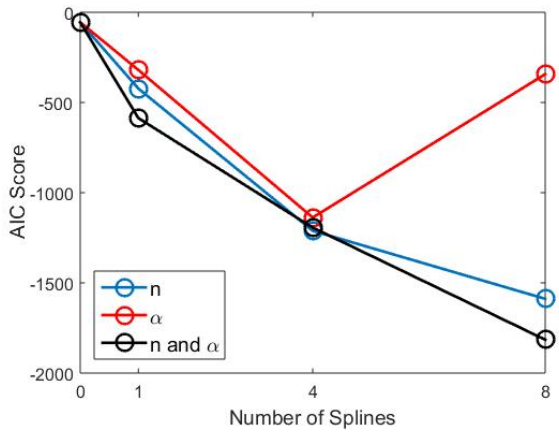


(b) Rat 2: AIC Scores

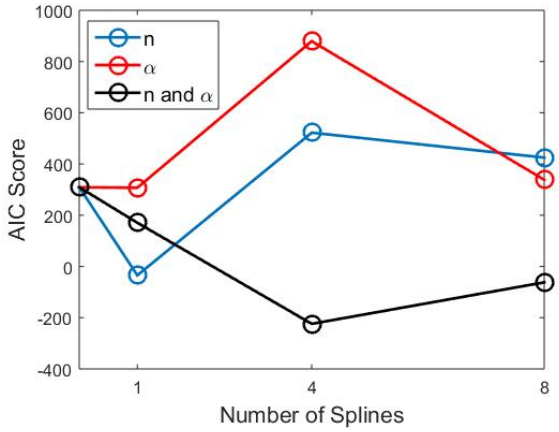


(c) Rat 3: AIC Scores

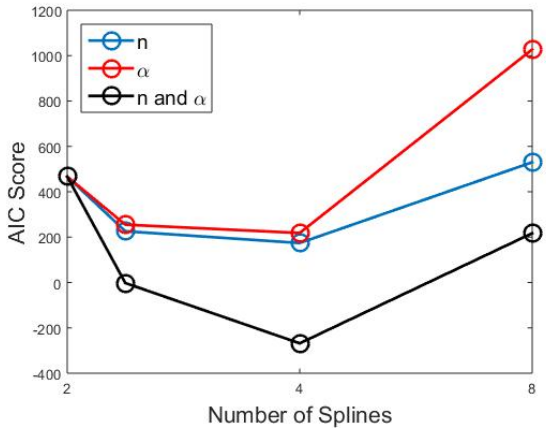


(d) Rat 4: AIC Scores

Figure 12: AIC Scores for Subjects 1-4 across models with time variation in combinations of $n$ and $\alpha$ for m = 1, 4, and 8 splines. Legend denotes which variable is time varying

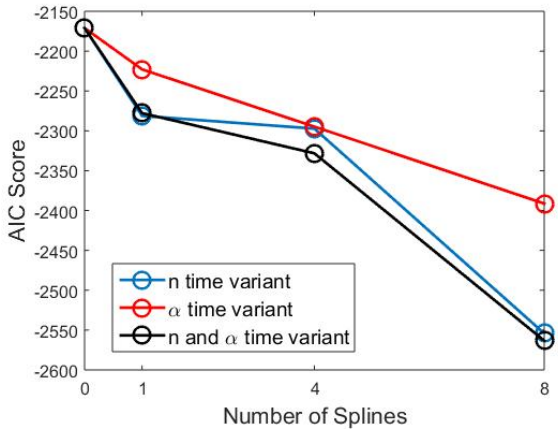


(a) Rat 5: AIC Scores

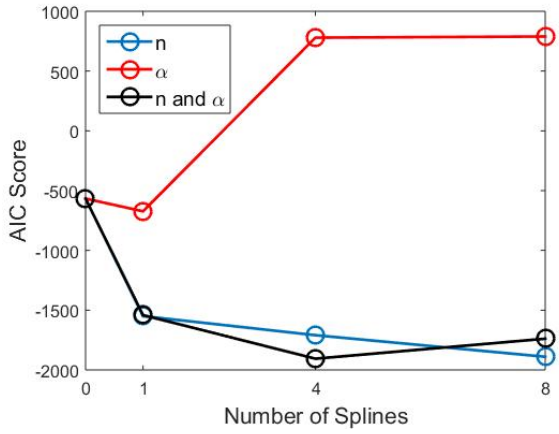


(b) Rat 6: AIC Scores

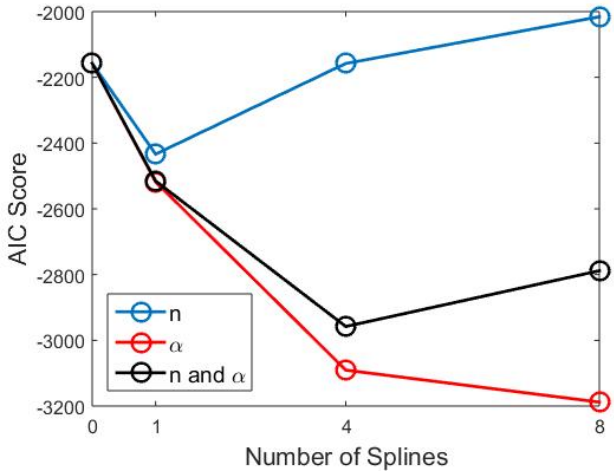


(c) Rat 7: AIC Scores

Figure 13: AIC Scores for Subjects 5-7 across models with time variation in combinations of $n$ and $\alpha$ for m = 1, 4, and 8 splines. Legend denotes which variable is time varying

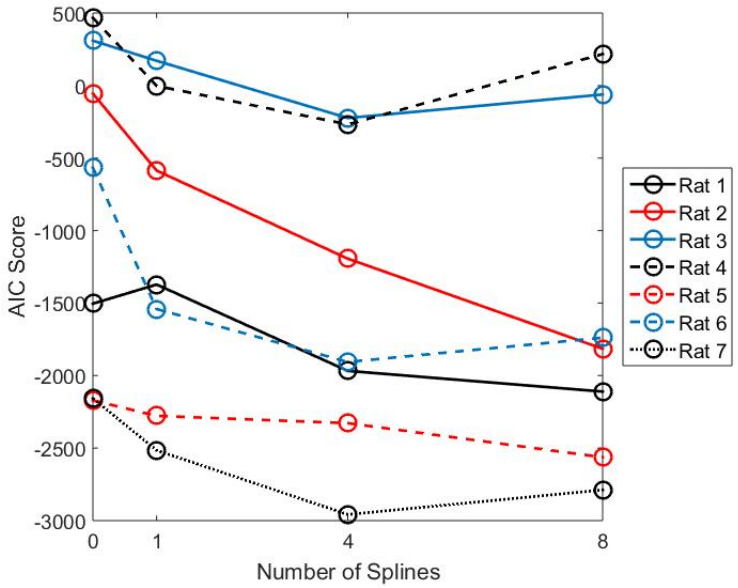


Figure 14: AIC Scores for all subjects using spline representations for $n$ and $\alpha$ as a function of the number of splines Used. The models using four and eight splines produce very similarly appropriate fits for many of the subjects

Table 2: P-values for nested model comparison tests for each rat. In each test, the first model listed is nested within the second, and a p-value of less than 0.05 indicates that the second model is significantly improved over the first. The model with four-spline representations of both $n$ and $\alpha$ is significantly superior to the constant model (Test 6), the one-spline models (Tests 7-9), and the four-spline models with either $n$ or $\alpha$ time varying (Tests 10-11). Introduction of eight-spline representations of $n$ and $\alpha$ does not offer significant improvement for 4 of the 7 rats (Test 12)

| Model Test | Rat 1 | Rat 2 | Rat 3 | Rat 4 | Rat 5 | Rat 6 | Rat 7 |
|---|---|---|---|---|---|---|---|
| 1) Constant vs $1n$ | 1.000 | 0.000 | 0.000 | 0.000 | 0.000 | 0.000 | 0.000 |
| 2) Constant vs $1\alpha$ | 1.000 | 0.000 | 0.046 | 0.000 | 0.000 | 0.000 | 0.000 |
| 3) Constant vs $1n/\alpha$ | 1.000 | 0.000 | 0.000 | 0.000 | 0.000 | 0.000 | 0.000 |
| 4) Constant vs $4n$ | 1.000 | 0.000 | 1.000 | 0.000 | 0.000 | 0.000 | 0.042 |
| 5) Constant vs $4\alpha$ | 0.000 | 0.000 | 1.000 | 0.000 | 0.000 | 1.000 | 0.000 |
| 6) Constant vs $4n/\alpha$ | 0.000 | 0.000 | 0.000 | 0.000 | 0.000 | 0.000 | 0.000 |
| 7) $1n$ vs $4n/\alpha$ | 0.000 | 0.000 | 0.000 | 0.000 | $1.85 \times 10^{-11}$ | 0.000 | 0.000 |
| 8) $1\alpha$ vs $4n/\alpha$ | 0.000 | 0.000 | 0.000 | 0.000 | 0.000 | 0.000 | 0.000 |
| 9) $1n/\alpha$ vs $4n/\alpha$ | 0.000 | 0.000 | 0.000 | 0.000 | 0.000 | 0.000 | 0.000 |
| 10) $4n$ vs $4n/\alpha$ | 0.000 | 1.000 | 0.000 | 0.000 | $1.23 \times 10^{-7}$ | 0.000 | 0.000 |
| 11) $4\alpha$ vs $4n/\alpha$ | 0.000 | $5.48 \times 10^{-14}$ | 0.000 | 0.000 | $1.02 \times 10^{-8}$ | 0.000 | 1.00 |
| 12) $4n/\alpha$ vs $8n/\alpha$ | 0.000 | 0.000 | 1.000 | 1.000 | 0.000 | 1.000 | 1.000 |

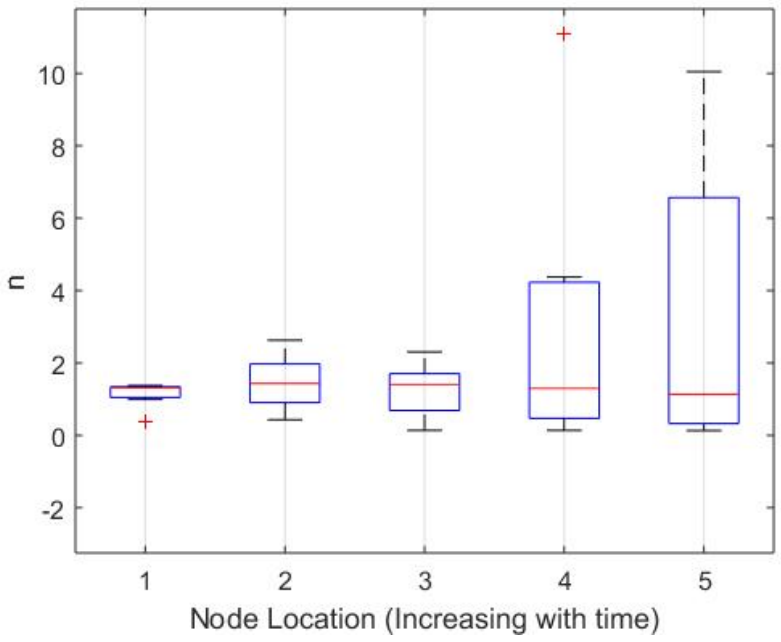


(a) Parameter: n

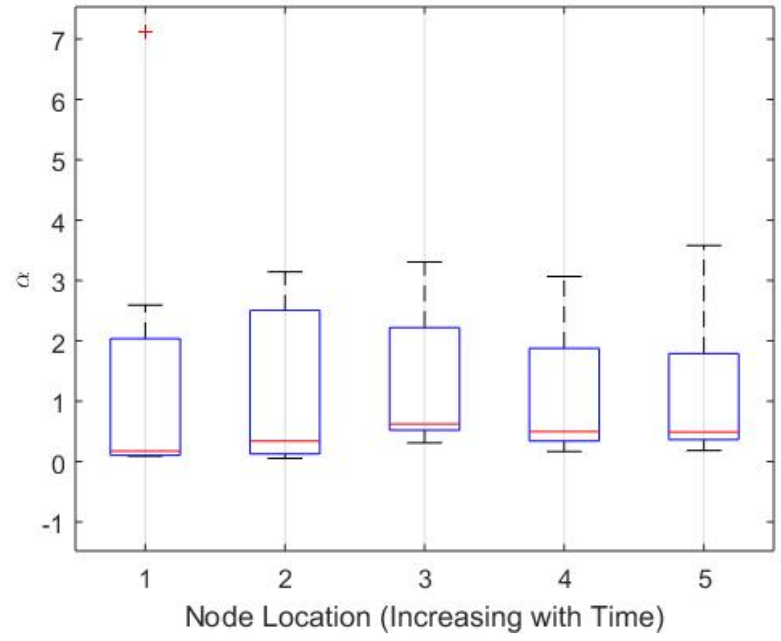


(b) Paramater: $\alpha$

Figure 15: Distributions of estimated node locations for four-spline representations of (a) $n$ and (b) $\alpha$ based on N = 7 subjects. Red lines represent median values; box boundaries define inner-quartile range (IQR); whiskers define min and max values within 1.5*IQR of median; red crosses denote outlying values

## 2.3 Discussion

The results of subset selection, which were previously mentioned, indicate that we do not possess sufficient information to estimate all six parameters listed in Table 1 with reasonable confidence. Of the three parameters we did not estimate (excluding $k_p$, which is perfectly correlated with $\alpha$), two contribute to the Hill equation for lipid dynamics ($EC_{50}$ and $E_{lip,max}$ in Equation 3), and the third describes the flow promoting effect of increasing the volume in the bloodstream ($K_{volume}$ in Equation 4). In retrospect, it is not surprising that we could not estimate $K_{volume}$ because without a control we cannot isolate the volume effect from the inotropic effect of the lipid. The same study by Fettiplace et al [16] from which we obtained lipid infusion data utilized a saline control infusion, but we did not have access to this data on an individual subject level. Likewise, estimation of $E_{lip,max}$ and $EC_{50}$ would be more feasible if our data had included multiple trials for each subject.

While unfortunate, these restrictions did not prevent us from achieving good fits via estimation of $n$ and $\alpha$. Akaike Information Criteria (AIC) scoring clearly indicates preference for the $n/\alpha$ models over the the Constant, $n$, and $\alpha$ models. (Figures 12-13). The results of the model comparison tests (Table 2) are consistent in this regard. Table 2 shows that the one-spline models are not consistently preferable to the constant estimate models, but that the $4n/\alpha$ model is significantly better than all constant and one-spline models. The exception noted by both AIC and model comparison is Rat 7 (Figure 13c and Test 11 in Table 2), for which the $4\alpha$ model provides the best fit. This outcome is likely due to the low peak (max $\approx$ 1.23 at 0.75 minutes) in cardiac output experienced by Rat 7 (Figure 9). We might postulate therefore that $n$ is the more critical parameter for capturing the magnitude of the cardiac response.

The flexibility conferred by the utilization of linear splines is apparent in Figures 3-9. Assumption of constant parameter estimates allows the model to fit relatively smooth responses with a single peak (Figures 3a and 7a), but irregular dynamics such as those exhibited in Figure 4a and 8a cannot be captured. The addition of a single spline representation significantly improves the tracking ability of the model, as Figures 4b and 8b attest. Even with time varying parameters, though, the model has difficulty fitting large initial peaks in relative cardiac output such as those experienced by Rats 3 and 4 (Figures 5 and 6). This limitation could be due to relying upon a population estimate for $E_{lip,max}$ (the parameter capturing the maximum effect of the lipid), rather than individual estimates. Including more splines does not resolve this issue, but it does allow the model to better detect sustained oscillations in the data (Figures 3, 7, and 9).

Of course, oscillation tracking may not be a desirable trait, as it is possible that the model is fitting noise rather than biologically relevant information. The spline representations of $n$ and $\alpha$ in Figures 10 and 11 can shed light on this matter. Ideally, we would prefer that the process of least squares estimation has not over-fit the data such that physiologically unreasonable or spuriously oscillatory parameter values are introduced. The first of those pitfalls does not appear to be an issue, as the respective estimates of $n$ and $\alpha$ at each node location (for all spline cases) are on the same order of magnitude as each other and as the population estimates reported by Fettiplace et al [14]. However, increasing the number of splines from four to eight introduces potentially meaningless (and large) oscillations in $n$ (Figures 10b and 10c). This trend is particularly apparent with respect to Rats 3 and 4, which we previously noted had large initial peaks in cardiac output. It is likely, therefore, that the spline approximation is estimating large and fast changes in $n$ in an unsuccessful attempt to model these peaks. The fact that $n$ is singled out for this purpose supports our earlier hypothesis concerning $n$ being the parameter

with greater influence on the magnitude of response.

The parameter $\alpha$, conversely, does not display biologically unreasonable behavior as the number of splines is increased from one to eight. The four and eight spline cases demonstrate ideal behavior in that the time varying parameters drift initially but converge towards what appear to be constant, baseline values (Figures 11b-11c). Rats 5 and 7, which had relatively lower estimates for $n$, demonstrated the largest $\alpha$ values compared to the other subjects. These two rats differ from the others in that they exhibit the two lowest initial peaks in relative cardiac output as well as sustained oscillations in cardiac activity throughout the time domain (Figures 7 and 9). The value of $\alpha$, therefore, could be the more important parameter with respect to the smoothness (or lack thereof) of cardiac response to lipid infusion. Though an eight-spline representation of $\alpha$ qualitatively appears reasonable, an equivalent representation of $n$ is not, likely making an eight spline model untenable.

Analyzing results from AIC and model comparison tests leads us along a similar chain of logic. Figure 14 confirms that introducing four-spline representations of $\alpha$ and $n$ consistently improves model performance over constant estimate and one-spline fits. However, doubling the number of splines from 4 to 8 results in a poorer model in four cases. Two of these instances follow from the model being unable to fit the maximum cardiac outputs experienced by Rats 3 and 4 (Figures 5-6), as discussed previously. Since the increase in model complexity does nothing to improve the fit, no reduction in AIC is accomplished. AIC scores also increased from the four-spline model to the eight-spline model for Rats 6 and 7, indicating that, though the fit visually appears improved, we over-fit the data in these two cases and do not capture meaningful information. The comparison test 12 in Table 2 identifies the same four rats as experiencing no significant benefit by increasing the number of splines from four to eight.

In consideration of these factors, the $4n/\alpha$ model represents the most appropriate choice for our study. Allowing time variation in $n$ and $\alpha$ renders the model capable of predicting dynamic individual responses to lipid emulsion infusion. By restricting the number of splines used for time variance, we achieve good fits to the available data without over-fitting or introducing unreasonable values or oscillations in our biological parameters. The process of model testing also provided insight as to the potential physiological roles of each parameter, with $n$ dictating the magnitude and shape of response and $\alpha$ serving as a smoothing factor.

# 3 Parameter Estimation 2

## 3.1 Methods

We recall that the results obtained above were constrained by insisting that splines be of equal length. That is, for example, a two-spline function for $n$ was composed of one line defined on the time interval $[0, 4.5]$ and another defined on $[4.5, 9]$. If we revisit Figures 10b and 11b, though, we see that neither parameter changes consistently across the time domain. The parameter $\alpha$ undergoes noticeable changes over the first 2 minutes but remains comparably constant over the final 7 minutes for all subjects. Likewise, each rat shows a contrast in the behavior of $n$ before and after 4 minutes.

We therefore desire to test if we can reduce the number of parameters in our model–while maintaining our model performance–by more judiciously selecting the node locations for each spline function. We introduce to our model a time vector $[0, 2, 9]$ containing the node locations for $\alpha$ and a time vector $[0, 4, 9]$ containing the node locations for $n$ (each node represents a time in minutes). Each parameter is thus described by two splines of unequal length. We solve the associated inverse problem in identical fashion as before.

## 3.2 Results

The model fits attained using unique two-spline representations of $n$ and $\alpha$ (denoted $2^*n/\alpha$ henceforth) are presented in Figures 16-22. For the purpose of comparison, the $1n/\alpha$ and $4n/\alpha$ fits are presented with each of the $2^*n/\alpha$ fits. We then calculate the AIC score associated with each new model and plot it along with the original models in Figures 23-24. Since the node locations are no longer consistent for all parameters, we cannot perform model comparison nested restraint tests. Thus, our sole quantitative metric for model selection will be AIC scores.

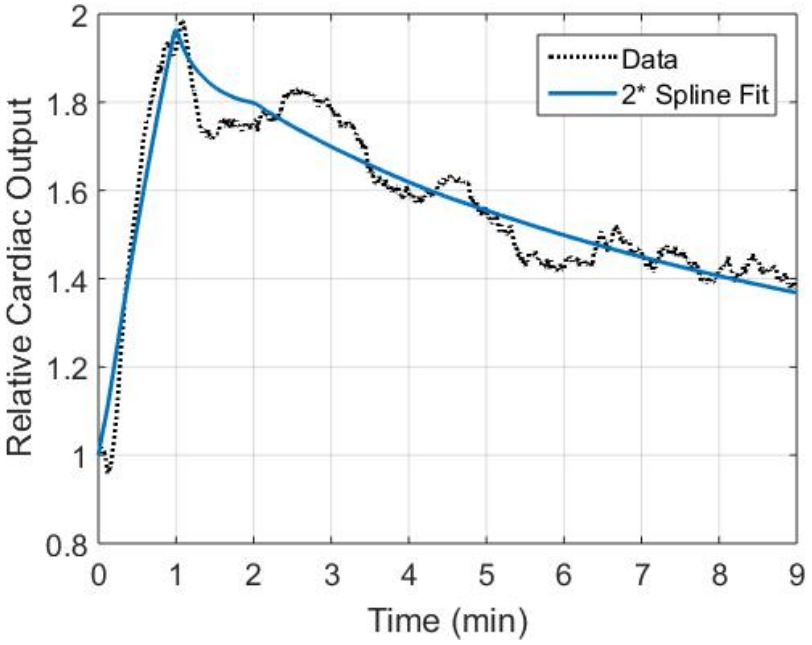


(a) Rat 1: m = 2* Splines

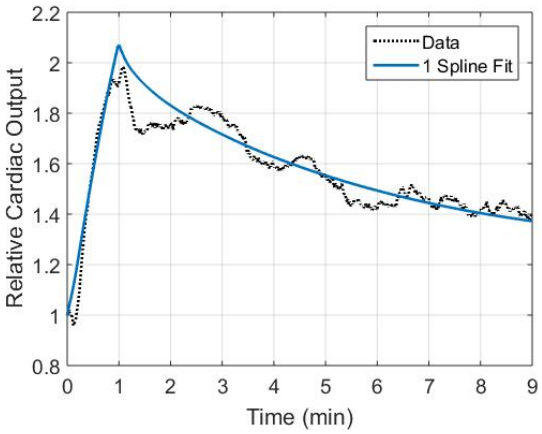


(b) Rat 1: m = 1 spline

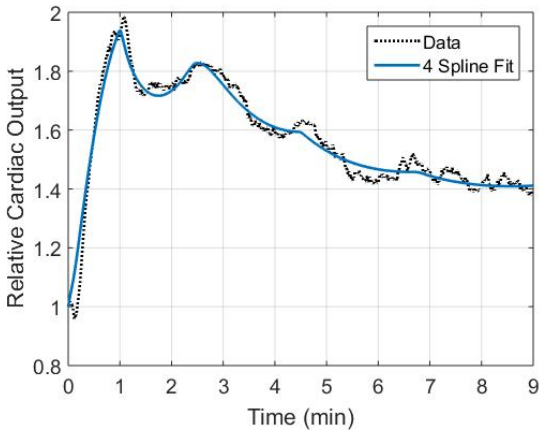


(c) Rat 1: m = 4 splines

Figure 16: Predicted cardiac output for rat 1 estimating $n$ and $\alpha$ as time varying parameters with (a) two splines of unequal length parameters compared to (b) one spline and (c) four splines of equal length

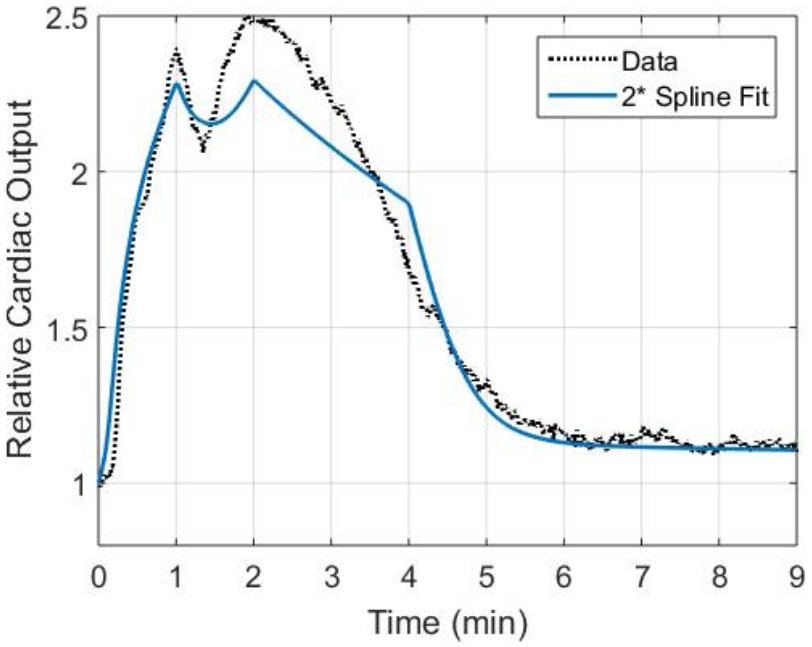


(a) Rat 2: m = 2* Splines

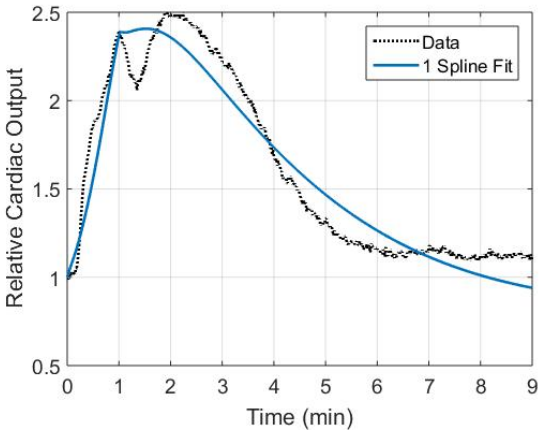


(b) Rat 2: m = 1 spline

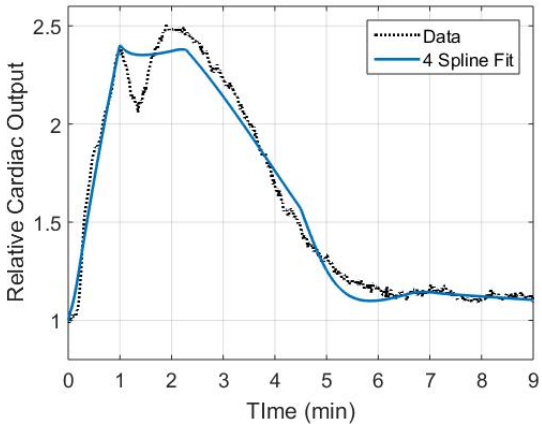


(c) Rat 2: m = 4 splines

Figure 17: Predicted cardiac output for rat 2 estimating $n$ and $\alpha$ as time varying parameters with (a) two splines of unequal length parameters compared to (b) one spline and (c) four splines of equal length

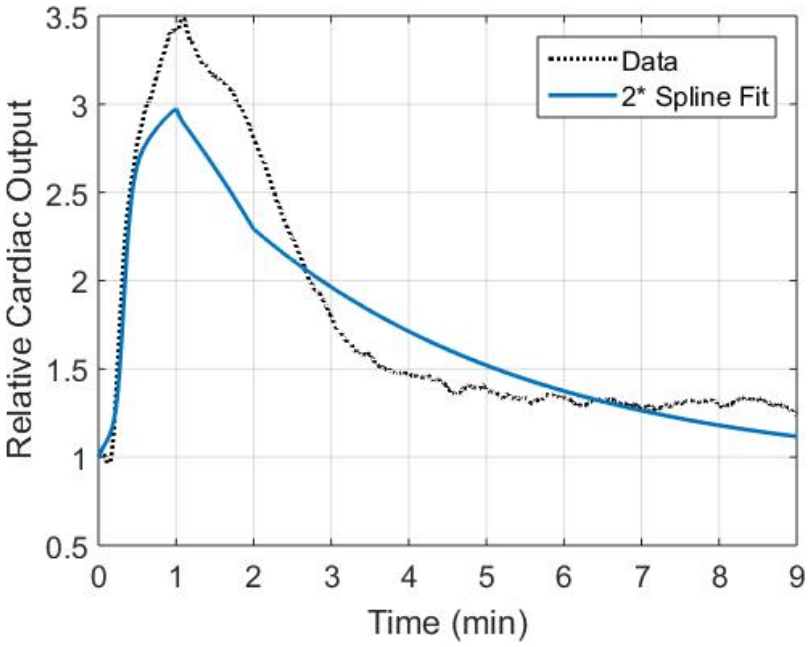


(a) Rat 3: m = 2* Splines

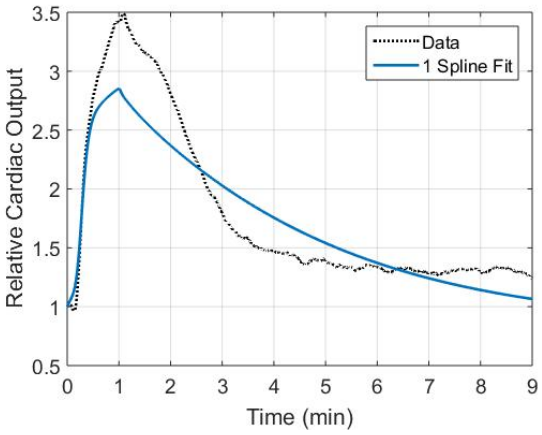


(b) Rat 3: m = 1 spline

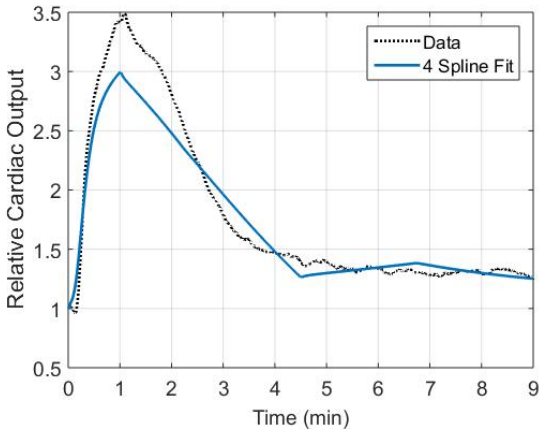


(c) Rat 3: m = 4 splines

Figure 18: Predicted cardiac output for rat 3 estimating $n$ and $\alpha$ as time varying parameters with (a) two splines of unequal length parameters compared to (b) one spline and (c) four splines of equal length

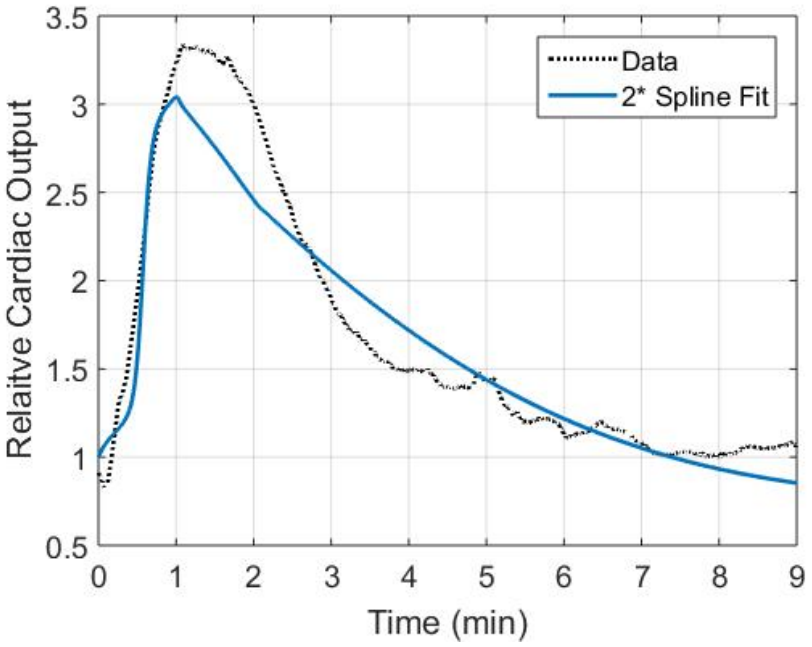


(a) Rat 4: m = 2* Splines

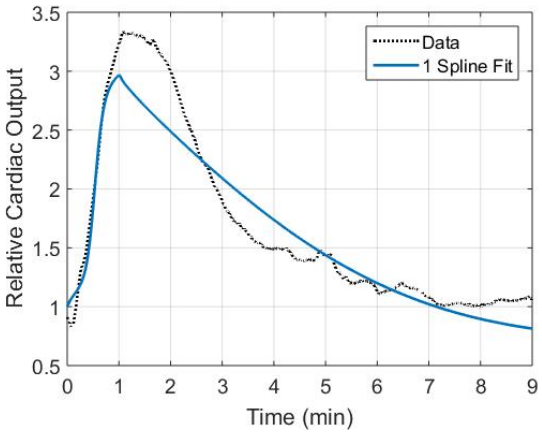


(b) Rat 4: m = 1 spline

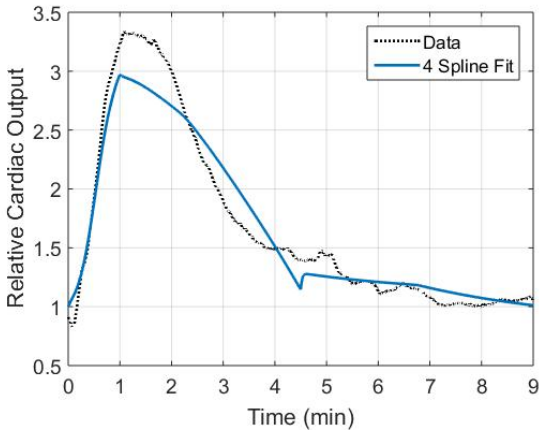


(c) Rat 4: m = 4 splines

Figure 19: Predicted cardiac output for rat 4 estimating $n$ and $\alpha$ as time varying parameters with (a) two splines of unequal length parameters compared to (b) one spline and (c) four splines of equal length

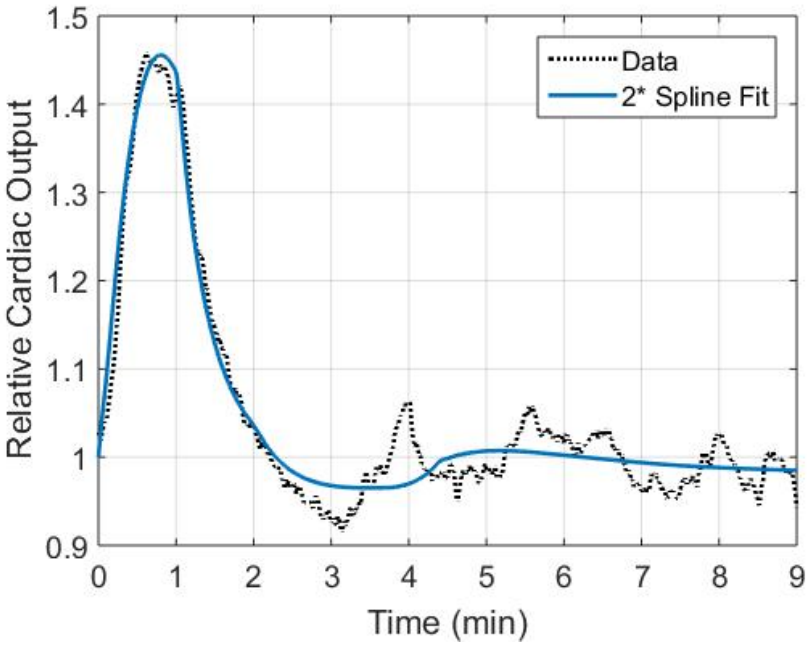


(a) Rat 5: m = 2* Splines

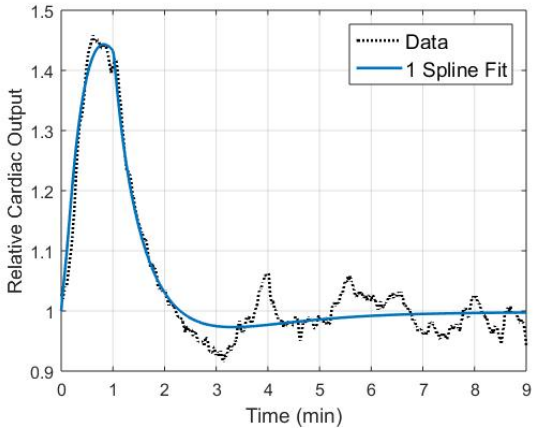


(b) Rat 5: m = 1 spline

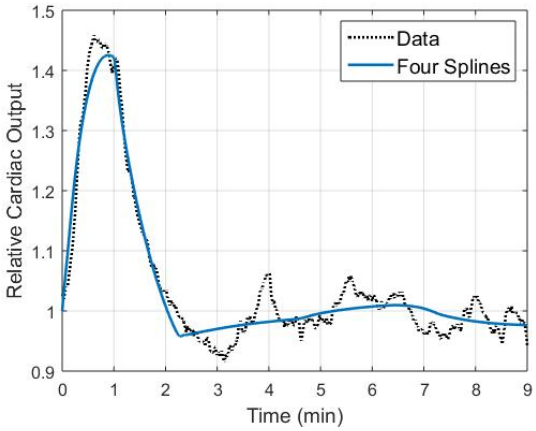


(c) Rat 5: m = 4 splines

Figure 20: Predicted cardiac output for rat 5 estimating $n$ and $\alpha$ as time varying parameters with (a) two splines of unequal length parameters compared to (b) one spline and (c) four splines of equal length

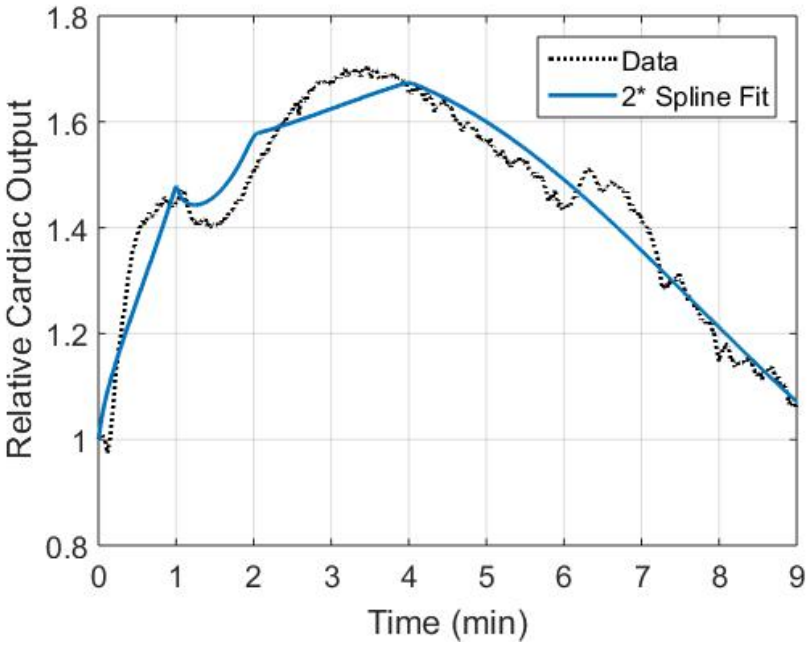


(a) Rat 6: m = 2* Splines

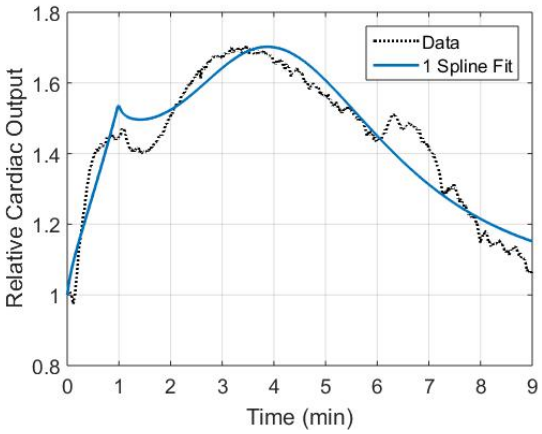


(b) Rat 6: m = 1 spline

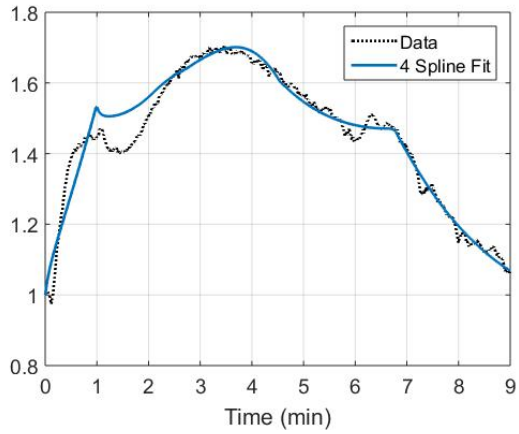


(c) Rat 6: m = 4 splines

Figure 21: Predicted cardiac output for rat 6 estimating $n$ and $\alpha$ as time varying parameters with (a) two splines of unequal length parameters compared to (b) one spline and (c) four splines of equal length

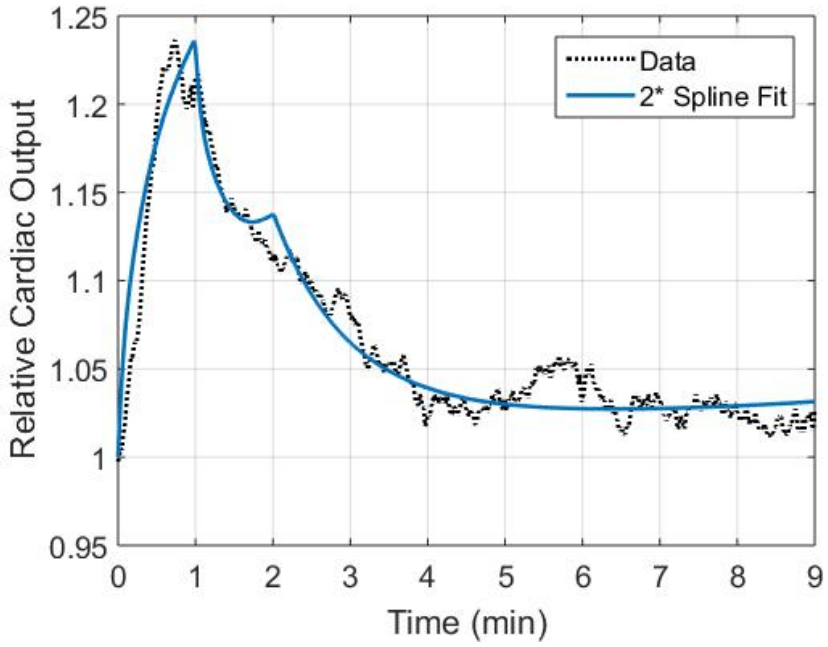


(a) Rat 7: m = 2* Splines

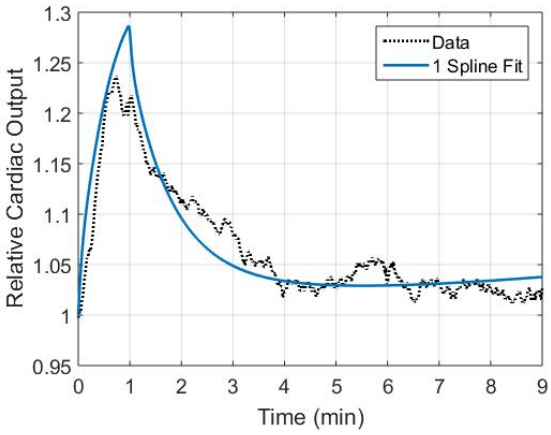


(b) Rat 7: m = 1 spline

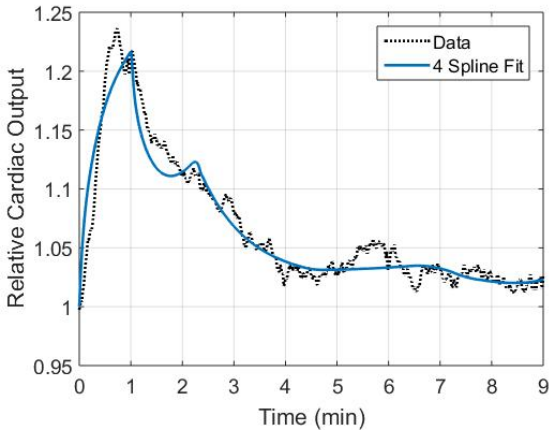


(c) Rat 7: m = 4 splines

Figure 22: Predicted cardiac output for rat 7 estimating $n$ and $\alpha$ as time varying parameters with (a) two splines of unequal length parameters compared to (b) one spline and (c) four splines of equal length

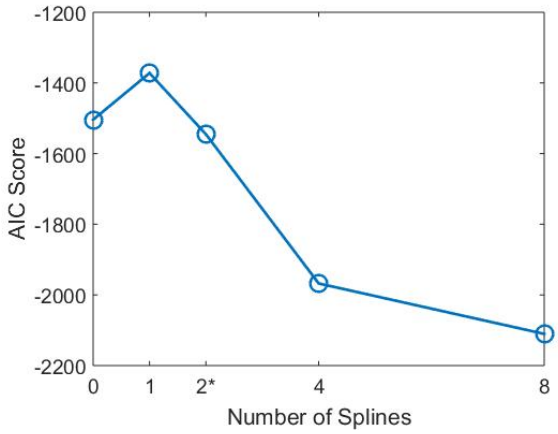


(a) Rat 1: Updated AIC Scores

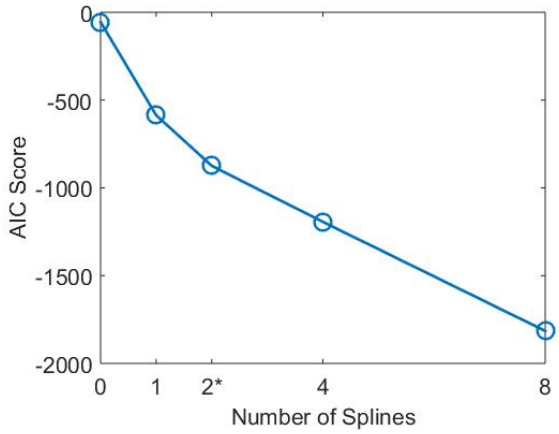


(b) Rat 2: Updated AIC Scores

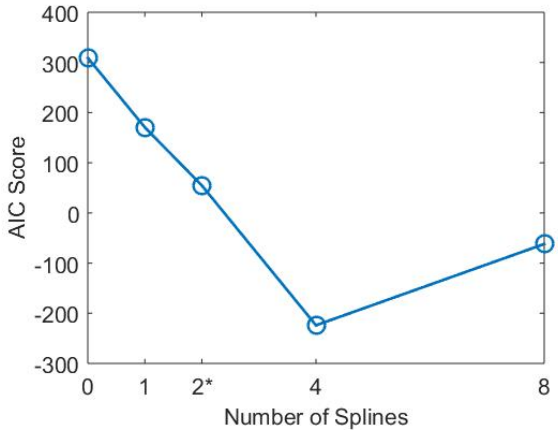


(c) Rat 3: Updated AIC Scores

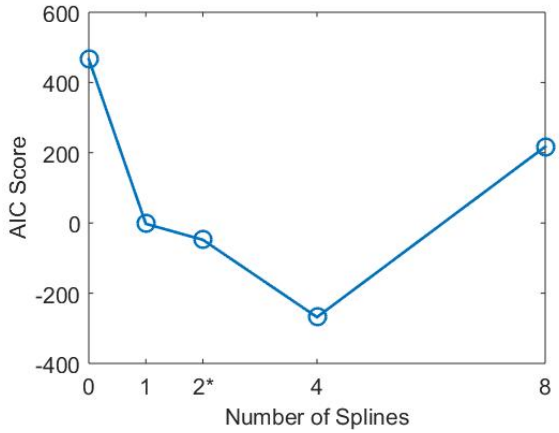


(d) Rat 4: Updated AIC Scores

Figure 23: AIC Scores for Subjects 1-4 across models with time variation in combinations of $n$ and $\alpha$ for m = 1, 4, and 8 splines. Updated to include model with 2 splines of unequal length ($2*$)

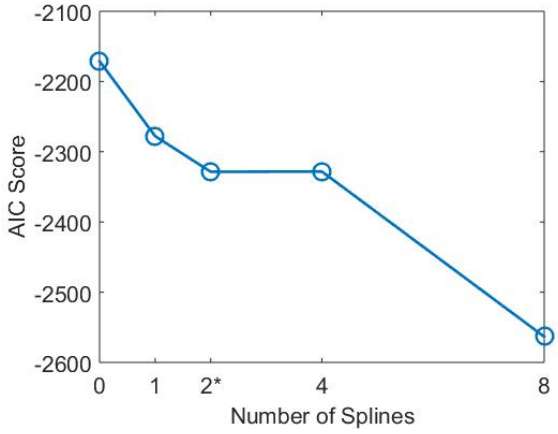


(a) Rat 5: Updated AIC Scores

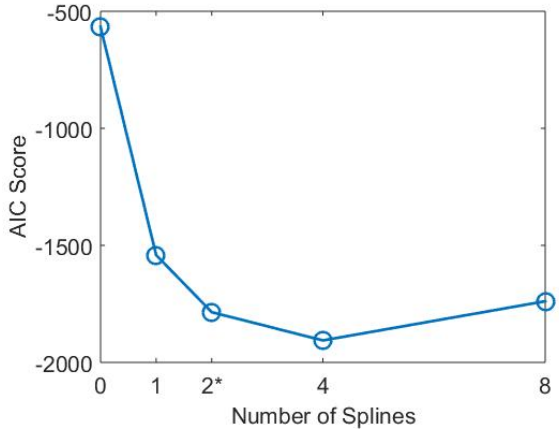


(b) Rat 6: Updated AIC Scores

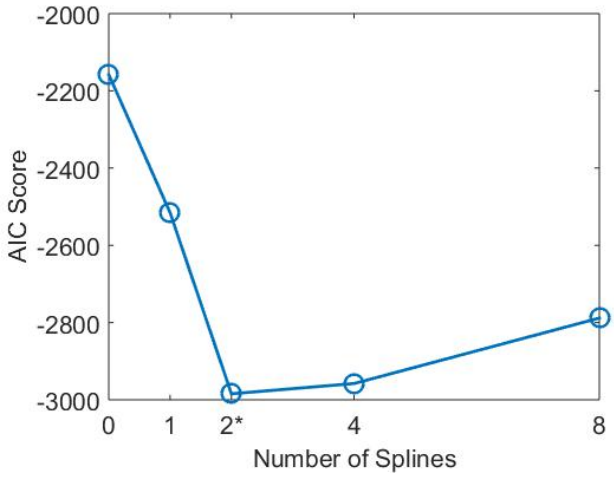


(c) Rat 7: Updated AIC Scores

Figure 24: AIC Scores for Subjects 5-7 across models with time variation in combinations of $n$ and $\alpha$ for m = 1, 4, and 8 splines. Updated to include model with 2 splines of unequal length ($2*$)

## 3.3 Discussion

The $2^*n/\alpha$ provides an interesting compromise between the $1n/\alpha$ and $4n/\alpha$ models. One shortcoming of the $4n/\alpha$ model is that, in some instances, the node placement causes the model to mistime a peak in cardiac output (see Figures 16c, 20c, 21c, and 22c). The analogous $2^*n/\alpha$ models (Figures 16a, 20a, 21a, and 22a) more accurately capture both the height of the maximums and the times at which they occur, which is a desirable trait. At the same time, the new model avoids the overshoot that is occasionally an issue with the $1n/\alpha$ models (Figures 16b and 22b) while preserving the ability to cut through the mean values of oscillatory regions rather than trying to track them exactly. This aspect may or may not be desirable, depending on the biological significance of those regions.

According to the weights assigned by AIC to these relative strengths and weaknesses, the $2^*n/\alpha$ model is not preferable to the $4n/\alpha$ model. The $2^*n/\alpha$ model, however, is useful to consider in future modeling efforts, particularly as we gain access to more data. If we are able to estimate more parameters, removing some of the data fitting burden from $n$ and $\alpha$, two carefully placed splines could prove sufficient to produce a model with high accuracy. Additionally, with only seven subjects, we do not have a firm grasp on what a typical response looks like. We might learn after collecting more data that we should not be overly concerned with the oscillations in cardiac output exhibited by some subjects. In such an event, the $2^*n/\alpha$ model would likely be the best choice. Since we are limited, though, to the information presently available, we will use the $4n/\alpha$ model for our virtual population study.

# 4 Virtual Population Studies

## 4.1 Methods

Based on the distributions of estimates for $n$ and $\alpha$ for our selected model (Figure 15), we elect to designate our parameters as belonging to log-normally distributed functions. We make this choice given that most of the box plots are right-skewed, particularly in the case of $\alpha$. The log-normal distribution is given by

$$X = e^{\mu+\sigma z} \tag{23}$$

Here, $X$ is a random variable whose natural logarithm has a normal distribution centered at $\mu$ with standard deviation $\sigma$ (z is the standard normal variable)[40]. The expected value and variance of $X$ are [40]

$$E(X) = e^{\mu+\frac{1}{2}\sigma^2} \tag{24a}$$

$$Var(X) = e^{2(\mu+\sigma^2)} - e^{2\mu+\sigma^2} \tag{24b}$$

We estimate the values $\mu$ and $\sigma$–which are sufficient to define a given distribution–for each parameter using the Matlab function *lognfit.m*.

Using these distributions, we construct virtual populations of rats undergoing two different ILE therapy regimens in response to LAST induced by intravenous absorption of bupivacaine. Bupivacaine overdose is modeled as a 10 mg/kg infusion administered at a constant rate for 20 seconds. Treatment with lipid is assumed to begin 10 seconds after completion of bupivacaine infusion. The two treatment regimens consist of 4 mg/kg of Intraplipid administered over 20 seconds, differing only in the percent lipid in the emulsion

(20% vs 30%). The anesthetic and treatment protocols are adopted from [14], which was a live animal study. Each virtual population consists of 10,000 individuals created by randomly sampling from our log-normal parameter distributions. The cardiac output of each "individual" is simulated using our PK/PD model. We use the 10,000 realizations to construct a median trajectory as well as the middle 50th and 95th percentiles.

## 4.2 Results

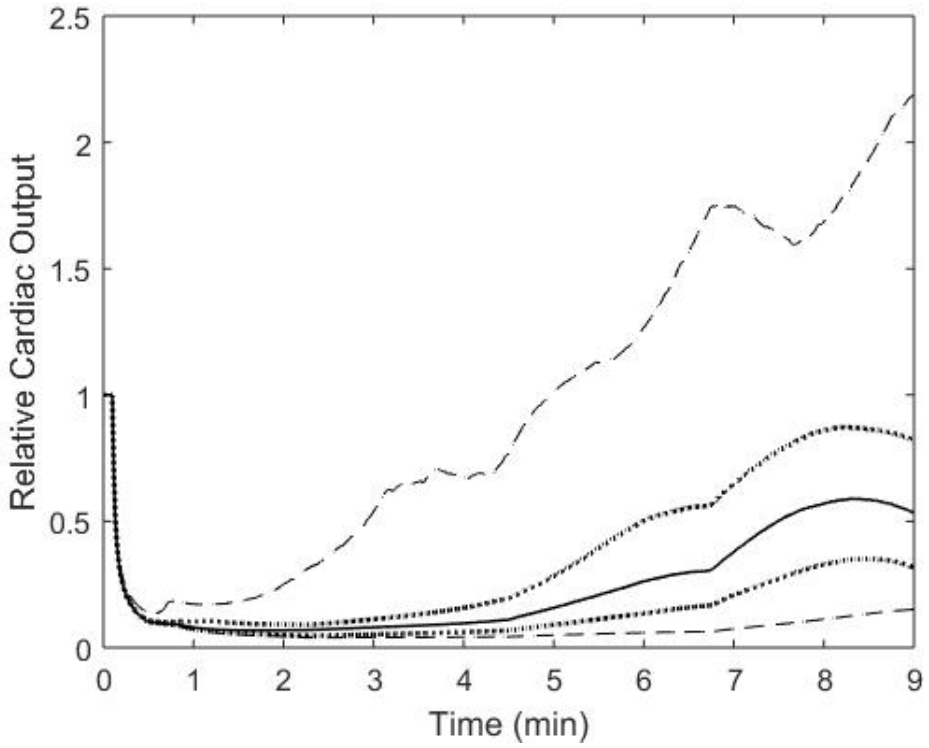


Figure 25: Virtual population of rats treated with 20% Intralipid in response to bupivacaine infusion using model with four-spline representations of $n$ and $\alpha$. Bupivacaine overdose modeled as 10 mg/kg administered at constant rate from time t = 0 to t = 20 seconds. Lipid treatment modeled as 4 mg/kg administered at constant rate from time t =30 to t = 50 seconds. Solid line = median, dotted lines = middle 50th percentile, dashed lines = middle 95th percentile

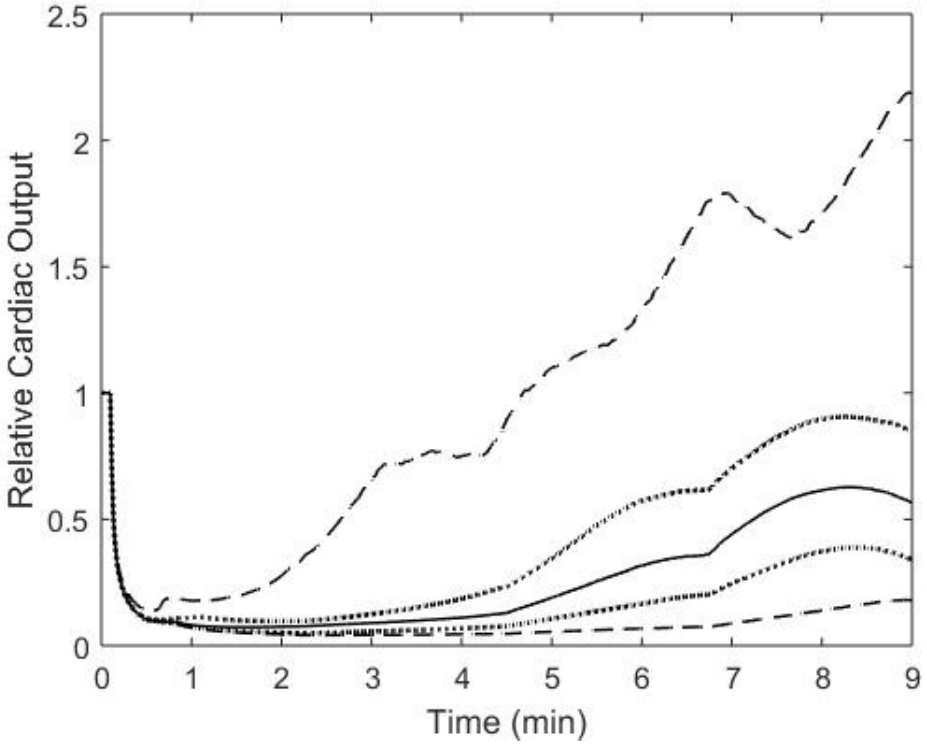


Figure 26: Virtual population of rats treated with 30% Intralipid in response to bupivacaine infusion. Bupivacaine overdose modeled as 10 mg/kg administered at constant rate from time t = 0 to t = 20 seconds. Lipid treatment modeled as 4 mg/kg administered at constant rate from time t =30 to t = 50 seconds. Black line = median, blue dotted lines = middle 50th percentile, red dashed lines = middle 95th percentile

## 4.3 Discussion

It is important to consider the limitations of our virtual population study. Our predictions are based solely on parameters estimated for a sample of seven rats. Thus, the distributions we obtained for $n$ and $\alpha$ may not necessarily be representative or well-defined. We individually estimated neither the volume effect parameter ($K_{volume}$), nor the maximum and half-max effect parameters ($E_{lip,max}$, $EC_{50}$) associated with lipid inotropy. Furthermore, the virtual study involves a bupivacaine infusion, introducing interactions for which we cannot account on an individual level with our lipid-only data. Had we possessed additional data to this effect, we could have estimated $EC_{50,bup}$ and $\beta$, the parameters associated bupivacaine response (Equation 2).

Having said that, we can still gain some preliminary insights from this virtual population. The wide variability in response, while certainly partially attributable to our sample size, confirms that we should not expect ILE therapy to be equally effective for all individuals. Such a thought is hardly revolutionary and should really follow intuitively, yet it is a point that has at times gotten lost in the rush to herald ILE therapy as the "silver bullet" against LAST. We also see that there is a small proportion of the population that is highly sensitive to lipid emulsion infusions and could experience spikes in cardiac output. Looking forward and assuming these results are generally accurate, we see that we have an avenue for establishing if a treatment is optimal at the population level.

Ideally, we would wish an average individual to show almost immediate improvement in cardiac function following ILE infusion and a return to baseline activity over the course of several minutes. We observe, however, that the average individual in our virtual population experiences only a return to 50% of baseline. Moreover, the initial response

to treatment is sluggish and cardiac function does not begin noticeably improving until approximately t = 4 (about 3 minutes after infusion of lipid). Our 50% confidence intervals reveal that approximately a quarter of the population will actually experience full recovery in the absence of any other intervention. We also see a potential reason to be cautious about attempting to model the oscillations in cardiac output present in the lipid-only data used for estimation. Our virtual population exhibits a tendency towards oscillatory behavior in the latter stages of treatment and, while such fluctuations may be relevant in lipid-only scenarios above cardiac baseline, we have no guarantee that they should exist at sub-baseline outputs in the presence of bupivacaine.

We can compare our results to the observations of Fettiplace et al [14], from whom we obtained the bupivacaine and ILE treatments prescribed in our virtual populations. The rats in that study achieved, on average, a return to baseline cardiac output in approximately five minutes. That is, the mean they reported nearly aligns with our 95% upper confidence limit, though with considerably less overshoot. We also did not observe as noticeable a difference between the responses of the 20% ILE and 30% ILE treatment groups (Figures 25 and 26 are imperceptibly different). One feature of their data that our model captures with the 95% upper confidence curve is an initial bump in recovery prior to the one minute mark. The timing of this local maximum is interesting as it occurs so quickly that it most likely due to a volume effect of the lipid rather than a sink effect. However, we did not observe this behavior in our mean response.

# 5 Conclusions and Future Work

We have demonstrated that we can use a physiologically based PK/PD model to characterize cardiac response to infusion of a lipid emulsion via estimation of relevant parame-

ters on an individual basis. Of the six parameter associated with lipid dynamics in the PK/PD model, we identified two parameters that could be estimated from the individual data: $n$, a Hill parameter for the inotropic action of the lipid, and $\alpha$, an auxiliary control parameter describing the action of homeostasis. We further established that treating $n$ and $\alpha$ as time varying parameters represented by linear spline functions rather than constants produced a better model fit to the data. That is not to say that we necessarily concluded that $n$ and $\alpha$ are time varying, but that we allowed them to assume the dynamic natures of the respective physiological processes which they represent. Model selection tests revealed that constructing the functions for $n$ and $\alpha$ with four splines of equal length was sufficient to produce reasonable fits without over-fitting noise or over-complicating the model. We also noted that, when estimating only these parameters, $n$ tended to define the magnitude of cardiac response while $\alpha$ smoothed or sharpened the response.

We assumed that population level distributions of our estimated parameters could be represented by log-normal distributions. By repeated random sampling from these distributions, we created a virtual population of subjects undergoing ILE therapy in response to an infusion of bupivacaine. The study demonstrated a wide range of expected outcomes, with approximately 25% of the population predicted to experience a return to baseline cardiac output via lipid intervention.

Future work with this model should focus on collecting sufficient data to individually estimate the volume effect parameter ($K_{volume}$) and the remaining lipid-effect parameters ($EC_{50}$, $E_{lip,max}$) that we left constant, as well as the bupivacaine response parameters ($EC_{50,bup}$ and $\beta$). This task could be achieved by administering multiple treatments in succession to a series of subjects: a saline treatment to isolate $K_{volume}$, a non-lethal bupivacaine-only treatment to establish $EC_{50,bup}$ or $\beta$ (or both), and a lipid-only treat-

ment. Given that our lipid-only treatment data could not identify three parameters (recalling that the fourth $k$, was perfectly correlated with $\alpha$), multiple rounds of lipid infusion with varying dosages would likely need to be performed. With this information we might gain a clearer picture as to which parameters are most influential in the mechanism of ILE action. Additionally, by performing multiple rounds of experimental dosages we would obtain data sets useful for validation of both our model and our virtual population estimates.

We should also consider expanding our modeling endeavors to higher animal models such as pigs or dogs, particularly given the inconsistent results that have been obtained in these species with respect to ILE therapy. Our model is flexible in that physiological parameters such as organ volumes, blood flow rates, etc. for different species can be easily imported. Estimation of parameters relevant to ILE could then be performed. Establishing mechanistic consistencies across multiple models would represent a significant step forward. Finally, once the model with lipid and bupivacaine has been thoroughly validated, we should introduce additional agents to our model such as vasopressors (the traditional treatment for LAST). In doing so, we could shed light on whether the interactions between ILE and vasopressors are synergistic, neutral, or antagonistic. While ambitious, these steps would greatly increase the clinical relevance of our model and move us closer to our ultimate goal: providing an informative resource that promotes both the safe and most effective application of ILE therapy.

# References


[1] George Albright. Cardiac arrest following regional anesthesia with etidocaine or bupivacaine. *The Journal of Anesthesiology*, 51(4):285–287, 1979.

[2] American College of Medical Toxicology. *Interim guidance for the use of lipid resuscitation therapy.*

[3] American Heart Association. *American Heart Association Guidelines for Cardiopulmonary Resuscitation and Emergency Cardiovascular Care*, 2015.

[4] H.T. Banks, Kidist Bekele-Maxwell, Lorena Bociu, Marcella Noorman, and Kristen Tillman. The complex-step method for sensitivity analysis of non-smooth problems arising in biology. Technical report, Center for Research in Scientific Computation, North Carolina State University, 2015.

[5] MJ Barrington and R Kluger. Ultrasound guidance reduces the risk of local anesthetic systemic toxicity following peripheral nerve blockade. *Reg Anesth Pain Med*, 38:289–297, 2013.

[6] Emma Bourne, Christine Wright, and Colin Royse. A review of local anesthetic cardiotoxicity and treatment with lipid emulsion. *Local and Regional Anesthesia*, 3:11–19, 2010.

[7] N. Buckley and A. Dawson. The intralipid genie is out of the bottle–spin and wishful thinking. *Anaesthesia and Intensive Care*, 41(2):154–156, 2013.

[8] Craig Clarkson and Luc Hondeghem. Mechanism for bupivacaine depression of cardiac conduction: fast block of sodium channels during action potential with slow recovery from block during diastole. *Anesthesiology*, 62(•):396–405, 1985.

[9] Thomas Coleman and Yuying Li. An interior trust region approach for nonlinear minimization subject to bounds. *Journal of Optimization*, 6(2):418–445, 1996.

[10] M. de Queiroz Siqueira, D. Chassard, H. Musard, A. Heilporn, J. Cejka, O. Leveneur, B. Allaouchiche, and O. Rhondali. Resuscitation with lipid, epinephrine, or both in levobupivacaine-induced cardiotoxicity in newborn piglets. *British Journal of Anaesthesia*, 112(4), 2014.

[11] Marc Van de Velde, Patrick Wouters, Norbert Rold, Hugo Van Aken, William Flameng, and Eugene Vandermeersch. Long-chain triglycerides improve recovery from myocardial stunning in concious dogs. *Cardiovascular Research*, 32:1008–1015, 1996.

[12] Hartmut Derendorf and Bernd Meibohm. Modeling of pharmacokinetic/pharmacodynamic (pk/pd) relationships: concepts and perspectives. *Pharmaceutical Research*, 16(1):176–185, 1999.

[13] Jean Eledjam, Jean de La Coussaye, Josep Brugada, Bruno Bassoul, Jean Gagnol, Juan Fabregat, Christian Masse, and Antoine Sassine. In vitro study on mechanisms of bupivacaine-induced depression on myocardial contractility. *Anesthesiology and Analgesia*, 69:732–735, 1989.

[14] Michael Fettiplace, Belinda Akpa, Richard Ripper, Brian Zider, Jason Lang, Israel Rubinstein, and Guy Weinberg. Resuscitation with lipid emulsion: dose-dependent recovery from cardiac pharmacotoxicity requires a cardiotonic effect. *Anesthesiology*, 120(4):915–925, 2014.

[15] Michael Fettiplace, Kinga Lis, Richard Ripper, Katarzyna Kowal, Adrian Pichurko, Dominic Vitello, Israell Rubinstein, David Schwartz, Belinda Akpa, and Guy Wein-

berg. Multi-modal contributions to detoxification of acure pharmacotoxicity by a triglyceride micro-emulsion. *Journal of Controlled Release*, 198(•):62–70, 2015.

[16] Michael Fettiplace, Richard Ripper, Kinga Lis, Bocheng Lin, Jason Lang, Brian Zider, Jing Wang, Israel Rubinstein, and Guy Weinberg. Rapid cardiotonic effecs ot lipid emulsion infusion. *Critical Care Medicine*, 41(8):156–162, 2013.

[17] Daniel Finkel. Direct optimization algorithm user guide. Technical report, Center for Research in Scientific Computation, North Carolina State University, 2003.

[18] G. Foxall, R. McCahon, J. Lamb, J.G. Hardman, and N.M. Bedforth. Levobupivacaine-induced seizures and cardiovascular collapse treated with intralipid. *Anaesthesia*, 62(516-518), 2007.

[19] Guido Di Gregario, David Schwartz, Richard Ripper, Kemba Kelly, Douglas Feinstein, Richard Minshall, Malek Massad, Carlo Ori, and Guy Weinberg. Lipid emulsion is superior to vasopressin in a rodent model of resuscitation from toxin-induced cardiac arrest. *Critical Care Medicine*, 37(3):993–999, 2009.

[20] M Harvey and G Cave. Lipid rescue: does the sink hold water? and other controversies. *British Journal of Anaesthesia*, 112(4):622–625, 2014.

[21] Shawn Hicks, David Salcido, Eric Logue, Brian Suffoletto, Phillip Empey, Samuel Poloyac, Donald Miller, Clifton Callaway, and James Menegazzi. Lipid emulsion combined with epinephrine and vasopressin does not improve survival in a swine model of bupivacain-induced cardiac arrest. *Anesthesiology*, 111:138–146, 2009.

[22] David Hiller, Guido Di Gregario, Richard Ripper, Kemba Kelly, Malek Massad, Lucas Edelman, Douglas Feinstein, and Guy Weinberg. Epinephrine impairs lipid resuscitation from bupicacaine overdose. *Anesthesiology*, 111(•):498–505, 2009.

[23] N.H.G Holford and L.B Sheiner. Kinetics of pharmacological response. *Pharmacology and Therapeutics*, 16:143–166, 1982.

[24] Leroy Hood and Stephen Friend. Predictive, personalized, preventative, participatory (p4) cancer medicine. *Nature Reviews: Clinical Oncology*, 8:184–187, 2011.

[25] Shuhua Hu. Akaike information criterion. Technical report, Center for Research in Scientific Computation, North Carolina State University, 2007.

[26] James Min-Che Huang, Hu Xian, and Marvin Bacaner. Long-chain fatty acids activate calcium channels in ventricular myocytes. *Proceedings of the National Academy of Science*, 89(•):6452–6456, 1992.

[27] William Jusko. Moving from basic towards systems pharmacodynamic models. *Journal of Pharmaceutical Sciences*, 102(9):2930–2940, 2013.

[28] David Kouba, Matteo LoPiccolo, Jeremy Bordeaux Murad Alam, Bernard Cohen, William Hanke, Nathaniel Jellinek, Howard Maibach, Jonathon Tanner, Neelam Vashi, Kenneth Gross, Trudy Adamson, Wendy Begolka, and Jose Moyano. Guidelines for the use of local anesthesia in office-based dermatologic surgery. *J Am Acad Dermatol*, 2016.

[29] Ilin Kuo and Belinda Akpa. Validity of the lipid sink as a mechanism for the reversal of local anesthetic systemic toxicity: a physiologically based pharmacokinetic model study. *Anesthesiology*, 118(6):1350–1361, 2013.

[30] Marilena Lekka, Stamatis Liokatis, Christos Nathanail, Vasiliki Galani, and George Nakos. The impact of intravenous fat emulsion administration in acute lung injurt. *American Journal of Respiratory and Critical Care Medicine*, 169:638–644, 2004.

[31] Michael Levine, Daniel Brooks, Aimee Franken, and Robert Graham. Delayed-onset seizure and cardiac arrest after amitriptyline overdose, treated with intravenous lipid emulsion therapy. *Pediatrics*, 130(2):432–438, 2012.

[32] Michael Levine, Aaron Skolnik, Anne-Michelle Ruha, Adam Bosak, Nathan Menke, and Anthony Pizon. Complications following antidotal use of intravenous lipid emulsion therapy. *Journal of Medical Toxicology*, pages 10–14, 2014.

[33] B. Li, J. Yan, Y. Shen, B. Li, Z. Hu, and Z. Ma. Association of sustained cardiovascular recovery with epinephrine in the delayed lipid-based resuscitation from cardiac arrest induced by bupivacaine overdose in rats. *British Journal of Anaesthesiology*, 108(5):857–863, 2012.

[34] Rainer Litz, Thomas Roessel, Axel Heller, and Sebastian Stehr. Reversal of central nervous system and cardiac toxicity after local anesthetic intoxication by lipid emulsion injection. *Anesthesia and Analgesia*, 106(5):1575–1577, 2008.

[35] Hugues Ludot, Jean-Yves Tharin, Mohamed Belouadah, Jean-Xavier Mazoit, and Jean-March Malinovsky. Successful resuscitation after ropivacaine and lidocaine-induced ventricular arrhythmia following posterior lumbar plexus block in a child. *Anesthesia and Analgesia*, 106(5):1572–1574, 2008.

[36] Jacqueline Mauch, Olga Martin Jurado, Nelly Spielmann, Regula Bettschart-Wolfensberger, and Markus Weiss. Resuscitation strategies from bupivacaine-induced cardiac arrest. *Pediatric Anesthesia*, 22, 2012.

[37] Viktoria Mayr, Lukas Mitterschiffthaler, Andreas Neurauter, Christian Gritsch, Volker Wenzel, Tilko Muller, Gunter Luckner, Karl Linder, and Hans-Ulrich Strohmenger. A comparison of the combination of epenephrine and vasopressin

with lipid emulsion in a porcine model of asphyxial cardiac arrest after intravenous injection of bupivacaine. *Anesthesia and Analgesia*, 106(5):1566–1571, 2008.

[38] Jean-Xavier Mazoit, Regine Le Guen, Helene Beloeil, and Dan Benhamou. Binding of long-lasting local anesthetics to lipid emulsions. *Anesthesiology*, 110:380–386, 2009.

[39] Felix Nadrowitz, Carsten Stoetzer, Nilufar Foadi, Jorg Ahrens, Florian Wegner, Angelika Lampert, Wolfgang Koppert, Jeanne de la Roche, and Andreas Leffler. The distinct effects of lipid emulsion used for "lipid resuscitation" on gating and bupivacaine-induced inhibition of the cardiac sodium channel nav1.5. *Anesthesiology and Analgesia*, 117(5):1101–1108, 2013.

[40] National Institution of Standards and Technology. *Engineering Statistics Handbook*.

[41] Joseph Neal, Christopher Bernards, John Butterworth, Guido Di Gregario, Kenneth Drasner, Michael Hejtmanek, Michael Mulroy, Richard Rosenquist, and Guy Weinberg. Asra practice advistory on local anesthetic systemic toxicity. *Reg Anesth Pain Med*, 35:152–161, 2010.

[42] H. Frederik Nijhout, Janet Best, and Michael Reed. Using mathematical models to understand metabolism, genes, and disease. *BMC Biology*, 13(79), 2015.

[43] Parisa Partownavid, Soban Umar, Jingyuan Li, Siamak Rahman, and Mansoureh Eghbali. Fatty-acid oxidation and calcium homeostatis are involved in the rescue of bupivacaine-induced cartiotoxicity by lipid emulsion in rats. *Critical Care Medicine*, 40(8):2431–2437, 2012.

[44] Jingmei Qiu. Interpolation by splines. Technical report, University of Houston, 2012.

[45] Meg Rosenblatt, Mark Abel, Gregory Fischer, Chad Itzkovich, and James Eisenkraft. Successful use of 20presumed bupivacaine-related cardiac arrest. *Anesthesiology*, 105:217–218, 2006.

[46] Leelach Rothschild, Sarah Bern, Sarah Oswald, and Guy Weinberg. Intravenous lipid emulsion in clinical toxicology. *Scandanavian Journal of Trauma, Resuscitation, and Emergency Medicine*, 18:51–59, 2010.

[47] Sebastian Stehr, Jorg Ziegeler, Annette Pexa, Reinhard Deussen, Thea Koch, and Matthias Hubler. The effects of lipid infusion on myocardial funtion and bioenergetics in l-bupivacaine toxicity in the isolated rat heart. *Regional Anesthesia*, 104(1):186–192, 2007.

[48] Michael Stemkovski, Robert Baraldi, Kevin Flores, and H.T. Banks. Green algae (raphidocelis subcapitata) growth model. Technical report, Center for Research in Scientific Computation, North Carolina State University, 2016.

[49] Daniell Turner-Lawrence and William Kerns II. Intravenous fat emulsion: A potential novel antidote. *Journal of Medical Toxicology*, 4(2), 2008.

[50] Guy Weinberg. Lipid emulsion infusion: resuscitation for local anesthetic and other drug overdose. *Anesthesiology*, 117(1):180–187, 2012.

[51] Guy Weinberg, Guido de Gregario, Richard Ripper, Kemba Kelly, Malek Massad, Lucas Edelman, David Schwartz, Narali Shah, Sophie Zheng, and Douglas Feinstein. Resuscitation with lipid versus epinephrine in a rat model of bupivacaine overdose. *Anesthesiology*, 108:907–913, 2008.

[52] Guy Weinberg, Richard Ripper, Douglas Feinstein, and William Hoffman. Lipid emulsion infusion resuces dogs from bupivacaine-induced cardiac toxicity. *Regional Anesthesia and Pain Medicine*, 28(3):198–202, 2003.

[53] Guy Weinberg, Timothy VadeBonecouer, Gopal Ramaraju, Marcelo Garcia-Amaro, and Micahel Cwik. Pretreament or resuscitation with a lipid infusion shift the dose response to bupivacaine-induced asystole in rats. *Anesthesiology*, 88:1071–1075, 1998.

[54] Xiaomei Zhuang and Chuang Lu. Pbpk modeling and simulation in drug research and development. *Acta Pharmaceutica Sinica B*, 6(5):430–440, 2016.